ANALYSIS OF SANDWICH WIRE ANTENNA CHARACTERISTICS

by

IBRAHIM A. HAROUN

A thesis
presented to the University of Manitoba
in partial fulfillment of the
requirements for the degree of
Master of Science
in
Electrical Engineering

Winnipeg, Manitoba, 1984

ANALYSIS OF SANDWICH WIRE ANTENNA CHARACTERISTICS

by

Ibrahim A. Haroun

A thesis submitted to the Faculty of Graduate Studies of the University of Manitoba in partial fulfillment of the requirements of the degree of

MASTER OF SCIENCE

ABSTRACT

The sandwich wire antenna has been studied in this thesis. The effect of an undulation conductor on the sidelobe level and the near field distribution is also investigated. Initially, the point source array theory has been applied to obtain an approximate expression for the array factor of this antenna. The validity of this approximate expression is examined by comparing the antenna patterns obtained using this simplified expression with the Numerical Electromagnetic Code (NEC). This comparison shows a good agreement. Using an approximate expression, the undulation heights are then determined to provide a Taylor near field distribution. The undulated line is subsequently studied using the NEC., to determine its near field and the radiation patterns. The near field is found to be different from the assumed Taylor distribution, but the sidelobes of its radiated field are generally acceptable. In practical, an iteration may be used to improve the near field distribution and subsequently the sidelobe levels of the far field pattern.

The characteristic impedance of the strip line, whereupon the undulated line is connected to the load, is obtained by using the finite difference method. The effects of various dielectric constants, the strip width, and the distance between the strip and the side walls of the trough, on the characteristic impedance and the relative wave velocity are also investigated.

ACKNOWLEDGEMENT

The author is grateful to Dr. L. Shafai of the Electrical Engineering Department, University of Manitoba, for suggesting the topic and his guidance, constant encouragement and constructive criticism through all phases of this work.

The valuable review of the entire manuscript by my wife, Mrs. Ellen Haroun, led to a number of clarifications and other improvements. It is a pleasure to thank my colleagues for their encouragement.

The financial support by Natural Sciences and Engineering Research Council of Canada and the Department of Electrical Engineering of the University of Manitoba is gratefully acknowledged.

CONTENTS

LIST OF TABLES

LIST OF FIGURES

Chapter 1

INTRODUCTION

The sandwich wire antenna was originally introduced by Rotman and Karas [1] in 1957, to overcome some of the mechanical disadvantages of the existing antennas used in radar engineering. Such antennas are normally large in size, to provide the required high gain, but the size results in excessive weight and large mounting and scanning structures. The sandwich wire antenna which is new is fabricated by printed circuit technology, thus resulting in a low profile and smaller weight.

The new sandwich wire antenna consists of three coplanar conductors of which the centre one, connected to the inner conductor of an unbalanced coaxial or strip transmission line feed, undulates in the form of sinusoidal, rectangular, triangular, or trapezoidal shapes. The two straight outer conductors are grounded to the external shield of the input. This antenna is usually terminated at the end so that a travelling-wave can be obtained. A detailed discussion of this antenna was given by Rotman and Karas [2] in 1959. The paper provided a clear description of the antenna behaviour, and presented experimental data on the attenuation of the current in the undulating conductor and the radiation patterns. It also indicated that load impedance mismatch caused continuous current reflections. An analysis of this antenna was

given by Chen [3]. His analysis was approximate, since he neglected the current attenuation along the central undulating conductor. However, his results were in close agreement with the experimental results of Rotman and Karas. In 1971, Green and Whitrow [4] analyzed the cavity backed geometry. They assumed a TEM wave excitation and showed that the radiation characteristics must be independent of the wire undulation geometry. The computed results agreed reasonably well with the experimental data.

The sandwich wire antenna has been considered by other investigators for designing light weight antenna arrays. Laverick and Welsh [5] have used a sinusoidal undulation and have achieved a -20 dB sidelobe level. Graham and Dawson [6] have used a trapezoidal undulation and have designed a 19 element array using a Taylor distribution. Their design was aimed at obtaining a -30 dB sidelobe level, but provided a sidelobe level of -25 dB. Hockham and Wolfson [7] have also designed planar arrays and have achieved around -26 dB sidelobe levels. Aboul-Atta and Shafai [8] have analyzed the sandwich wire antenna as a boundary value problem and derived the attenuation constant, which provides essential information for the design of the sandwich wire antenna. The calculation of the characteristic impedance of the sandwich wire antenna with a central undulated line is difficult, since it is a three dimensional structure. However, from a practical point of view, the calculation of the undulated line impedance is not necessary. This is due to the fact that the central undulated line is normally connected to both the generator and the load,

through a straight section of the line. The impedance matching at these terminal points can therefore be achieved, using the characteristic impedance of three parallel conductors [9].

The previous work reported on the sandwich wire antennas have utilized either experimental procedures, or approximate analyses to study or design such antennas.

The purpose of this thesis is to extend our understanding of these antennas by utilizing more accurate analytic and numerical methods to study the various electrical properties of these antennas , such as the current and near field distribution and radiation patterns in the case of both end-fed and centre-fed. It is also the intention to develop a design procedure to determine the antenna dimensional parameters to meet certain specified electrical characteristics. The thesis consists of five chapters including the introduction.

Chapter II gives an approximate expression for the array factor of the sandwich wire antenna. Since the radiation from the sandwich wire antenna is thought to be due to the sections of the line which are perpendicular to the array axis, the undulated line can be represented by discrete radiating elements. Using this simplifying expression of the array factor for different numbers of elements and neglecting the attenuation constant along the array, the sidelobe level is found to be around -13 dB. This is an expected result from the well-known array theory [29], since a uniformly excited, equally-spaced linear array has -13 dB sidelobe level. The numerical modeling of the sandwich wire an-

tenna is also investigated. By using a search method, the optimum value of the load impedance is determined, which minimizes the end reflections. For a 13 element array, the numerically obtained results gave the first sidelobe level at approximately -14.0 dB. The difference between this result and the result of the discrete linear array is due to the fact that the numerical solution includes the effect of the attenuation along the array. The similarity of the two results was established by introducing a proper attenuation constant (α = 0.22 nepers/meter) along the array and calculating its array factor. The approximate expression using the discrete array theory helps in understanding the radiation from the antenna and enables one to use the well known array theories (Dolph-Chebyshev and Taylor's line source methods) to design antennas with better radiation characteristics.

Chapter III explains the design of tapered sandwich wire antennas. The model which is considered represents a tapered undulated wire above the ground plane. This model is excited at the centre and its ends are loaded by load resistances to assist in establishing a travelling-wave along the structure. To achieve a low sidelobe level, a Taylor's distribution [10] is used to determine the undulation geometries. Only the rectangular undulation shape is considered and the numerical electromagnetic code is used to compute the current distributions and the radiation patterns. The effect of varying the frequency and the height of the undulation, on the antenna sidelobe levels, is also investigated. The antenna is designed to have -40 dB sidelobe levels

but the designed unit normally yields results around -32 dB when it is fed at the centre. The reason for this difference will be explained later on in the chapter.

Chapter IV presents the numerical calculation of the characteristic impedance and the relative wave velocity of a straight conductor inside a trough, whereupon the undulated line can be connected to the required circuit elements. The characteristic impedance and relative wave velocity are computed by using a finite difference method for solving the Laplace Equation for the domain defined by the inner and outer conductors of Figs. 4.1-4.2. A computer program to solve the difference equations is prepared which calculates the line impedance for any trough and line shape, as well as the dielectric substrate dimensions. Using this program, the line characteristic impedance and relative wave velocity are computed for different substrate and line parameters. The results are presented graphically and can be used as design data.

Chapter V contains some concluding remarks about the main characteristics of the sandwich wire antenna.

Chapter II

ARRAY FACTOR OF SANDWICH WIRE ANTENNA

2.1 INTRODUCTION

The operation of the sandwich wire antenna can be explained by considering a transmission line consisting of a central conductor mounted between two side walls of a trough as shown in Fig.2.1 [11]. When the central conductor is parallel to the side walls, the energy propagates along the line in the guided strip line mode. No radiation takes place because the currents in the wires are travelling in opposite directions at intervals of half wavelengths and thus the radiation from each half wavelength is in anti-phase and cancels out [12]. Any tendency for incomplete cancellation can be suppressed by extending the side walls in front of the centre conductor, to form a cut-off wave guide for waves which are polarized parallel to them. However, if the line is undulated with respect to the side walls with an undulation of one wavelength as shown in Fig.2.2, the current components perpendicular to the side walls are all in the same direction, and radiation results. The undulating wire is supported on a thin dielectric strip, and is fabricated by using the printed circuit technique [13],[14]. In this chapter, the resulting radiation patterns (Array Factor) of the sandwich wire antenna will be investigated.

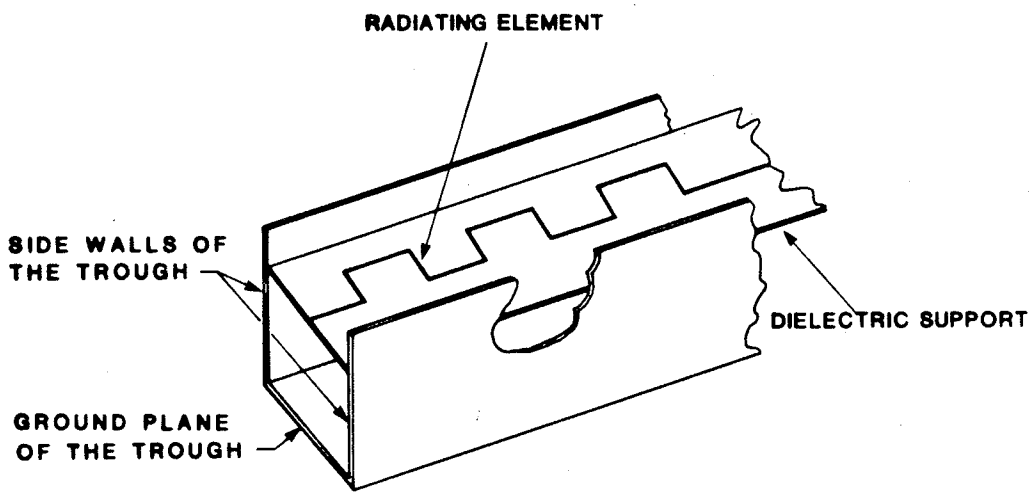

FIG. 2.1 SANDWICH WIRE ANTENNA

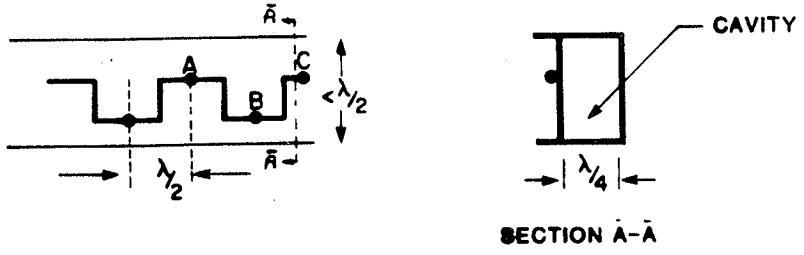

FIG. 2.2 PLANE VIEW AND CROSS-SECTION OF THE UNDULATED CONDUCTOR INSIDE THE TROUGH

2.2 ARRAY FORMED FROM UNDULATED LINE

Since only the elements perpendicular to the side walls radiate, they can be considered as elements of a discrete array [4], The phase of the radiating elements can be determined by their spacing along the transmission line [15], and the array factor can be determined to study the antenna radiation patterns. Using this approach, two different cases are considered in this chapter:

1) End-fed array, where the undulated line is excited at one end.
2) Centre-fed array, where the undulated line is excited at the centre.

Each case is studied separately and their radiation patterns are computed to determine their expected sidelobe levels.

2.2.1 End Fed Linear Array

In this case, the undulated line is terminated at one end, and the other end is connected to the source, as shown in Fig. 2.3 , so that a travelling wave can be launched. If the lengths AB and BC are half-wavelength, the current distributions along the vertical sections radiate in phase. For a travelling wave current along the structure the current I along the structure can be assumed as [3]

$$I = I_0 e^{-(\alpha + j\beta)\ell} \qquad (2.1)$$

where

α is the attenuation constant.

I_o is the input current at the generator terminal.

ℓ is the distance along the structure.

β is the phase constant along the structure.

In this analysis, we consider the broadside radiation. Hence, the interelement phase shift ψ is given by

$$\psi = \beta d \cos \phi$$

where,

$\beta = 2\pi/\lambda$

ϕ is the angle between the axis of the array and the vector from the origin to the observation point.

d is the distance between the radiating elements.

λ is the wavelength.

Assuming the radiation of each element to be due to a single point at the centre of the vertical sections, the array factor of the antenna can be shown to be [29]

$$AF = 1 + e^{j(\Psi + j\alpha\ell)} + e^{j2(\Psi + j\alpha\ell)} + ... + e^{j(N-1)(\Psi + j\alpha\ell)} \quad (2.2)$$

Assuming

$$Z = e^{j\omega}$$

$$\omega = \Psi + j\alpha\ell$$

equation (2.2) can be reduced to [29]

$$AF = e^{j\{(N-1)/2\}\,\omega} \left[\frac{\sin(\frac{N}{2}\omega)}{\sin(\frac{\omega}{2})} \right] \quad (2.3)$$

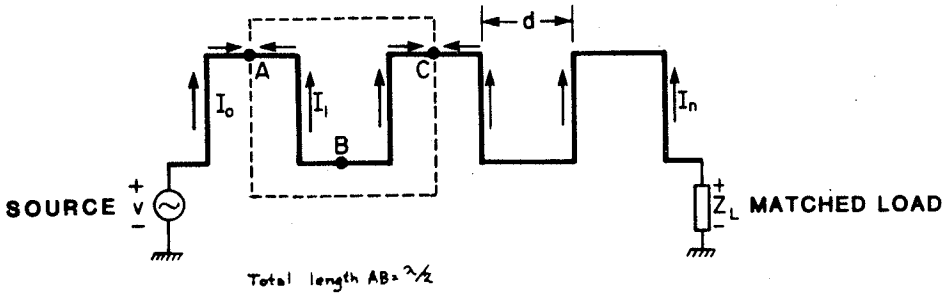

FIG.2.3 CURRENT DISTRIBUTION ON UNDULATED WIRE

END-FED

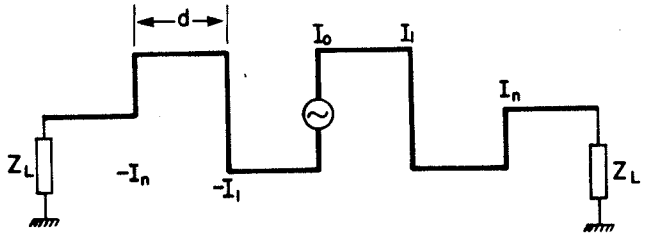

FIG.2.4 UNDULATED WIRE ANTENNA

CENTRE-FED

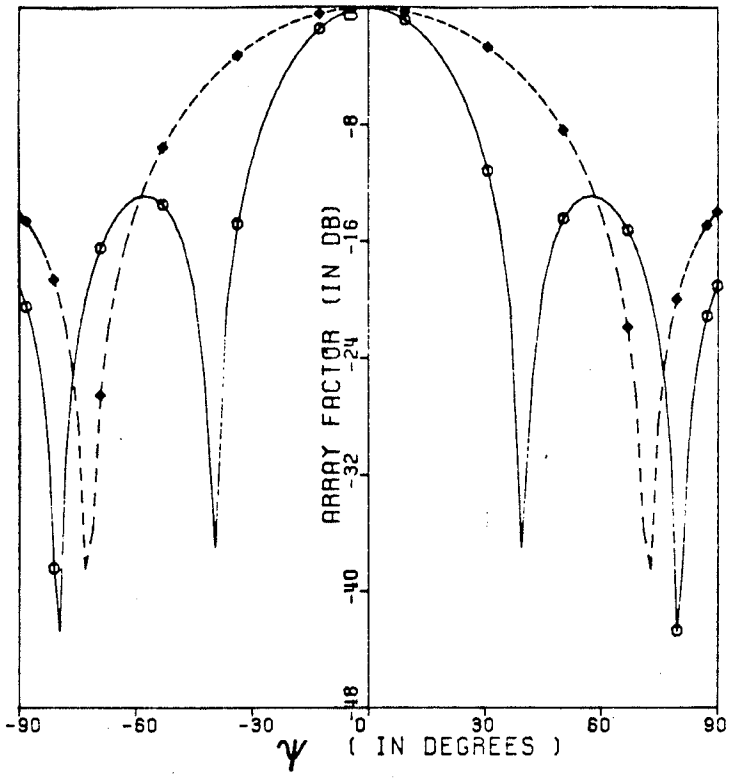

FIGURE 2.5 ARRAY FACTOR OF AN END-FED SANDWICH WIRE ANTENNA APPROXIMATED BY ARRAY FACTOR OF UNIFORM POINT SOURCES

⊙ —— 7 ELEMENTS

◆ ----- 4 ELEMENTS

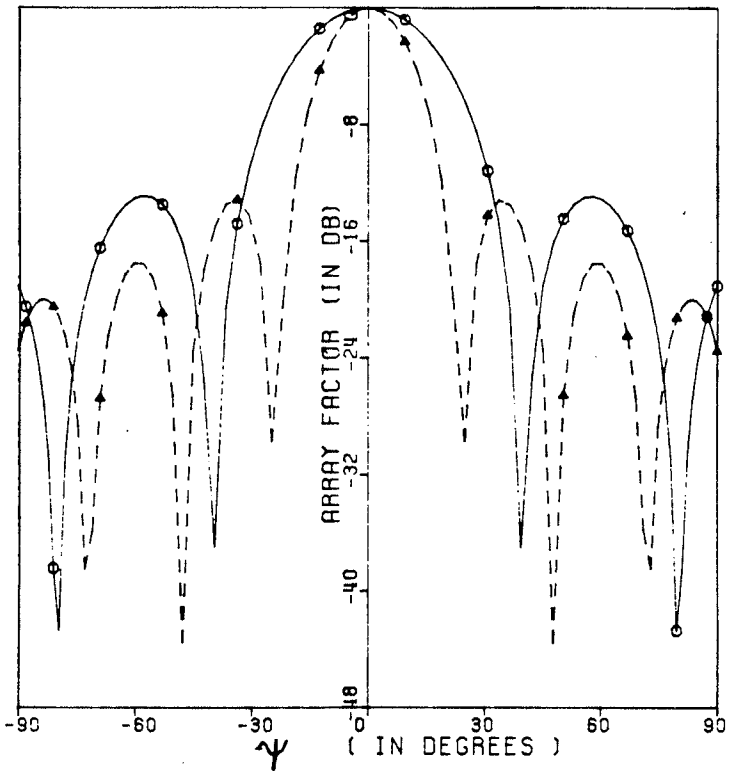

FIGURE 2.6 ARRAY FACTOR OF AN END-FED SANDWICH WIRE ANTENNA APPROXIMATED BY ARRAY FACTOR OF UNIFORM POINT SOURCES

⊙ —— 7 ELEMENTS

▲ ----- 10 ELEMENTS

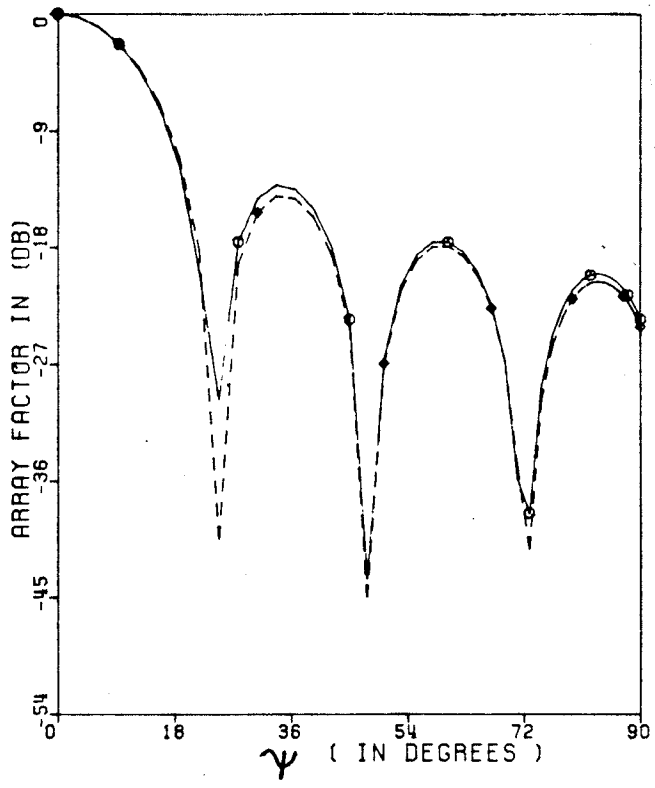

FIGURE 2.7 ARRAY FACTOR OF AN END-FED SANDWICH WIRE ANTENNA APPROXIMATED BY ARRAY FACTOR OF UNIFORM POINT SOURCES

◆ 10 ELEMENT α=0.10

⊙ 10 ELEMENT α=0.0

This expression can be used to extract information about the beam width, the location of pattern nulls, and the sidelobe levels of the array pattern. For different number of elements and neglecting the attenuation constant, the plots of this expression are shown in Figs. 2.5-2.6. From these results, the first sidelobe level in all cases is found to be about -13.3 dB below the main beam. This is a well known result from a uniformly-excited equally-spaced linear array. This sidelobe level is too high for many directive antenna applications, such as in radar and direction finding. From Fig. 2.7, when the attenuation constant along the array is increased to α=0.10, the first sidelobe level is reduced to -13.9 dB. Hence, the sidelobe level can be reduced to some extent by tapering the amplitude of the excitation of the elements [9],[10]. This possibility will be discussed in detail in chapter III. Figs. 2.5-2.6 also indicate that the pattern beam width can be reduced by increasing the number of radiating elements. The radiation characteristics can therefore be controlled easily in these antennas.

2.2.2 Centre Fed Linear Array

Most of the earlier work which has been carried out on the sandwich wire antenna considers feeding of the array at one end [1-9]. However, if the line losses are significant, some improvement in the efficiency can be obtained by feeding the array at the centre as shown in Fig. 2.4. In this case, the efficiency increases, since the input power is now inserted where the ampli-

tude distribution is maximum. Assuming that the amplitude excitation of the radiating elements is symmetrical about the array centre, the array factor will be given by

$$AF = 2 + e^{-\alpha\ell}\, e^{j\Psi} + \ldots + e^{-(N-1)\alpha\ell}\, e^{j(N-1)\Psi} + e^{-\alpha\ell}\, e^{-j\Psi} + \ldots + e^{-(N-1)\alpha\ell}\, e^{-j(N-1)\Psi} \tag{2.4}$$

which can be reduced to the form.

$$AF = 2 \sum_{n=1}^{N} e^{-(n-1)\alpha\ell} \cos\left[(n-1)\,\frac{2\pi}{\lambda}\, d \cos\phi\right] \tag{2.5}$$

The pattern of this array factor is shown in Fig. 2.8 when the attenuation along the array is neglected.

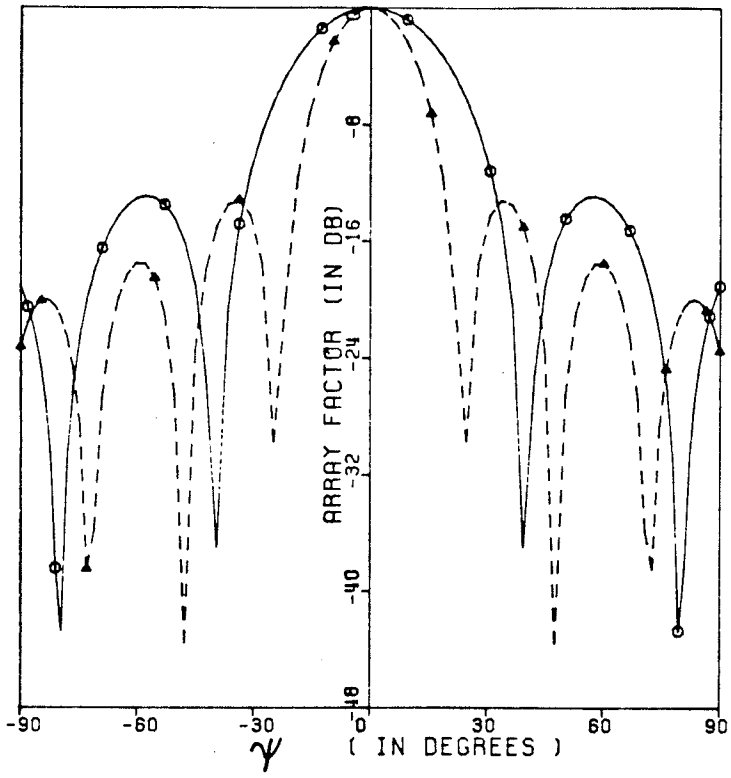

FIGURE 2.8 ARRAY FACTOR OF AN CENTRE-FED SANDWICH WIRE ANTENNA APPROXIMATED BY ARRAY FACTOR OF UNIFORM POINT SOURCES

⊙ —— 7 ELEMENTS

▲ ----- 10 ELEMENTS

2.3 NUMERICAL MODELLING

Sandwich wire antennas of practical size are difficult to model for numerical computation. The main difficulty is with the side walls of the trough, which require a large number of sub-areas and excessive storage memories. The other difficulty is with the dielectric card that generates polarization currents. The undulated centre wire can be modelled using the wire approximation [33]. The side walls can be modelled either by the surface patch method or by the wire grid approximation [33]. Both require approximately the same amount of computer storage. In the wire grid approximation the wire segment length should be less than 0.1 wavelength. Thus if the length of the sandwich wire is 25 λ , the total number of wire segments that are required to model the side walls of height $\lambda/4$, is in excess of 1000. For the undulated wire one may use 250 wire segments, which means the total wire segments will exceed 1250. Since the current distribution on each wire segment is unknown and must be obtained from a matrix solution, the matrix dimension will exceed 1250 X 1250. The solution of this matrix requires excessive storage memories and long execution time. In addition, the inversion of a large matrix due to excessive computation, causes the accumulation of round-off errors that makes the the solution inaccurate. Due to these difficulties, the model is considered as an undulated wire above the ground plane. This model is used to determine the current distribution and its phase variation along the undulating wire. One of its advantages is that it models only the undulating centre wire and thus requires reasonable computer storage and time.

2.3.1 Matching the Undulated Wire

Since the sandwich wire antenna is a travelling wave antenna, any reflection from its ends affects its radiation characteristics. It is therefore essential to eliminate such reflection by terminating its end in a matched load [1]. To search for a matched load a straight wire segment of length 3 λ is selected and assumed to be at a distance $\lambda/4$ over the ground plane as shown in Fig. 2.9(a) to 2.9(b). At the left end of the wire, a voltage source is used to excite the wire and the other end is connected to the ground through a load resistance. The value of this resistance should be equal to the characteristic impedance of the wire to achieve a reflection free termination. This characteristic impedance can be determined approximately using the expression for the characteristic impedance of two infinite parallel lines which is given by [29]

$$Z_o = \frac{138}{\sqrt{\varepsilon_r}} \log_{10}(4\,\frac{h}{d}) \qquad (2.6)$$

where

d= the diameter of the wire.

h= the height from the ground plane.

Z_o= the characteristic impedance.

ε_r= the dielectric constant.

The impedance computed by this equation can be used as starting point for determination of the optimum matched load for the an-

tenna. This can be achieved by adjusting the size and location of the required load, until a lowest standing wave on the line is obtained. Following the above procedure, equation 2.6 was used with $d = 0.004\ \lambda$, $h = 0.25\ \lambda$ and $\varepsilon_r = 1$ to compute the starting resistance value which is 330.9 ohms. Using this resistance as the load, the current distribution on the conducting wire was determined using the Numerical Electromagnetic Code (NEC). Its results are shown in Fig. 2.9 (a). Since the current exhibits a significant standing wave character, the size and location of the load resistance are changed to search for their optimum combination. The results are shown in Figs. 2.9(a) and 2.9(b) which indicate that a load resistance of 200 ohms may be used as a matched load. This load resistance is used in all computations of this thesis to reduce the end reflections.

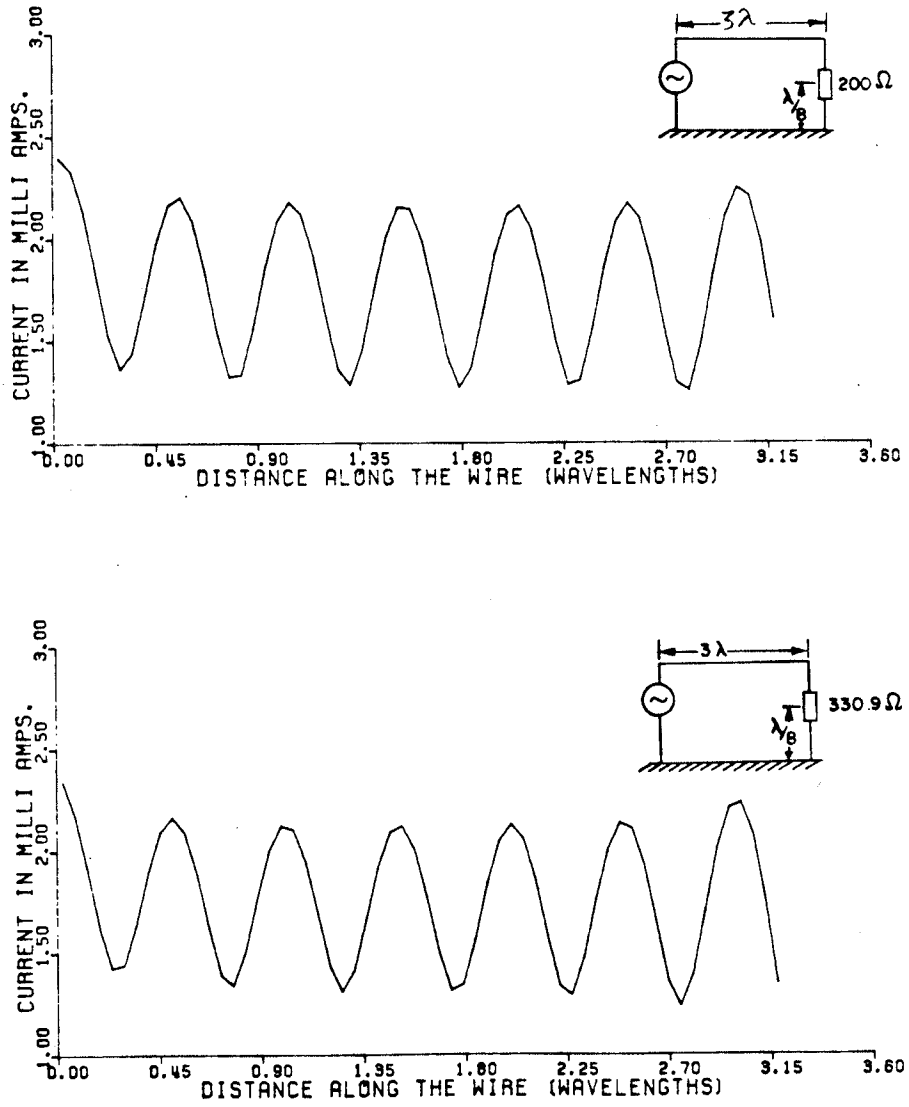

FIG.2.9(a) CURRENT DISTRIBUTION ALONG STRAIGHT WIRE FOR DIFFERENT LOAD

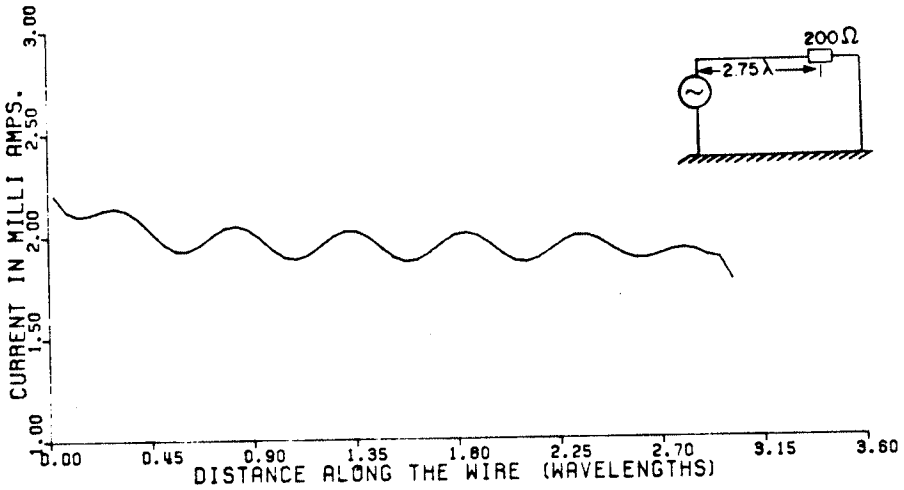

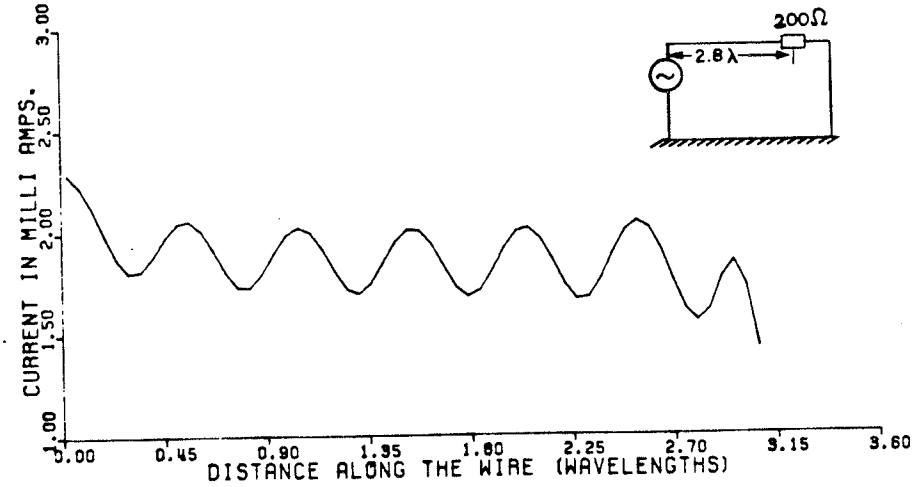

FIG.2.9(b) CURRENT DISTRIBUTION ALONG STRAIGHT WIRE FOR DIFFERENT LOCATION

2.4 VALIDITY OF APPROXIMATE ANALYSIS

To verify the validity of the approximate expression of the array factor for the sandwich wire antenna developed in section 2.2, the Numerical Electromagnetic Code [31-32] is used to study the radiation characteristics of a uniform undulated rectangular antenna. The undulated line is mounted at a distance $\lambda/4$ above the ground plane, and terminated by a 200 ohms load through a straight segment section of a length 0.75 λ. The amplitude and phase of the current distributions of this antenna for different heights are shown in Figs. 2.10,2.11,2.12. From these curves, it can be seen that when the undulation height increases, the attenuation increases. Since the attenuation is due to the radiation, the radiation increases with the undulation height. The radiation patterns of the undulated antenna for two different heights are calculated by using NEC and shown in Figs. 2.13-2.14. From Fig.2.13, the first sidelobe level is about -14.8 dB below the main beam, when the height of the undulated line is 0.15 wavelength, and becomes -14.03 dB when the height is reduced to 0.1 wavelength as shown in Fig. 2.14. These sidelobe levels are different from the well-known result of the discrete array, since the numerical solutions include the attenuation along the antenna. By determining the attenuation constants along the array for the two different heights (0.15 λ and 0.1 λ), and including these attenuations in the expression of the array factor, the radiation patterns for the two different heights are shown in Figs. 2.13-2.14. The results of these figures indicate that the radia-

tion patterns, calculated using the simplified array factor approach, can represent the actual antenna patterns, when a proper attenuation constant is selected. The main difference between the results of the numerical solution and the array factor approach is the location of pattern nulls, which is due to the fact that the designed antenna resonates at a somewhat lower frequency, and this will cause phase error along the array.

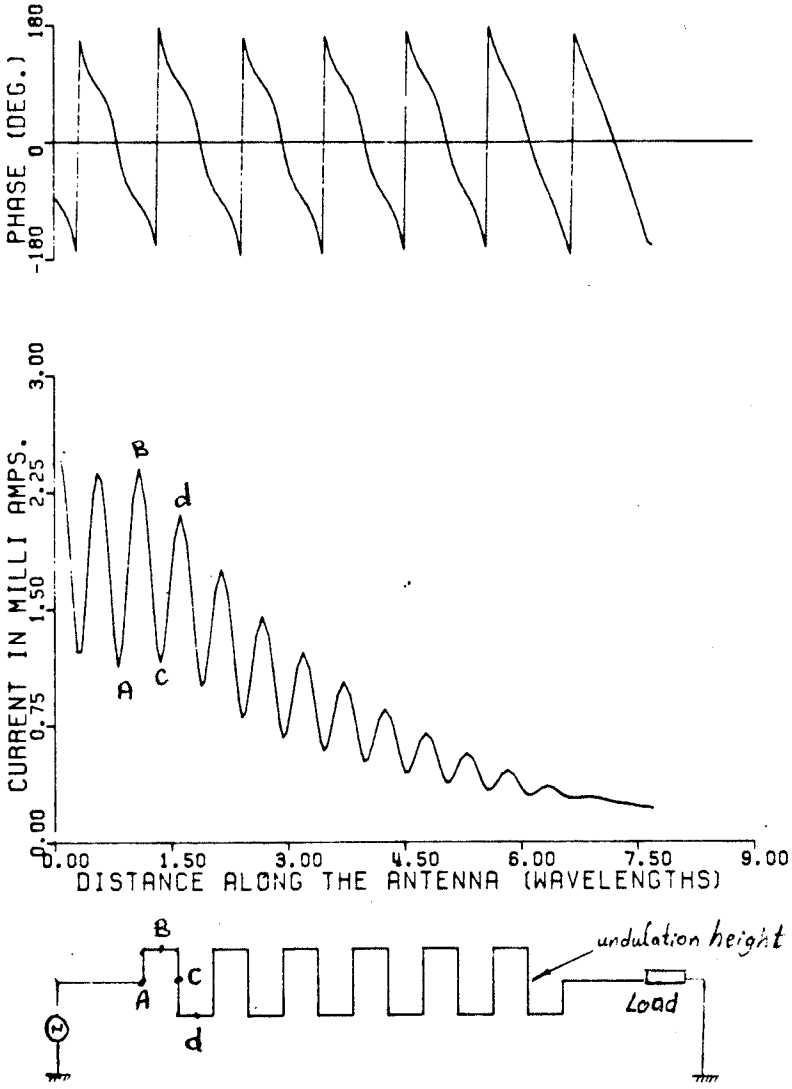

FIG. 2.10 PHASE AND CURRENT DISTRIBUTIONS ALONG THE UNDULATED WIRE

HEIGHT OF THE ELEMENT 0.20 WAVELENGTH

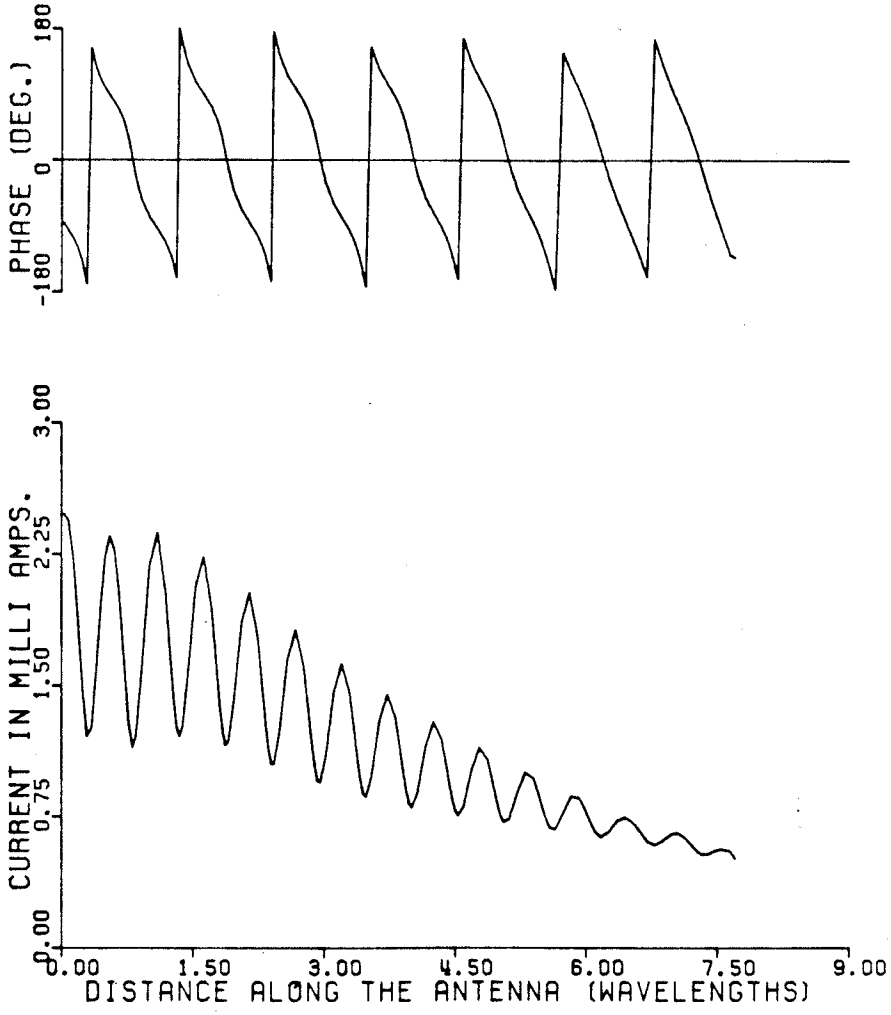

FIG. 2.11 PHASE AND CURRENT DISTRIBUTIONS ALONG THE UNDULATED WIRE

HEIGHT OF THE ELEMENT 0.15 WAVELENGTH

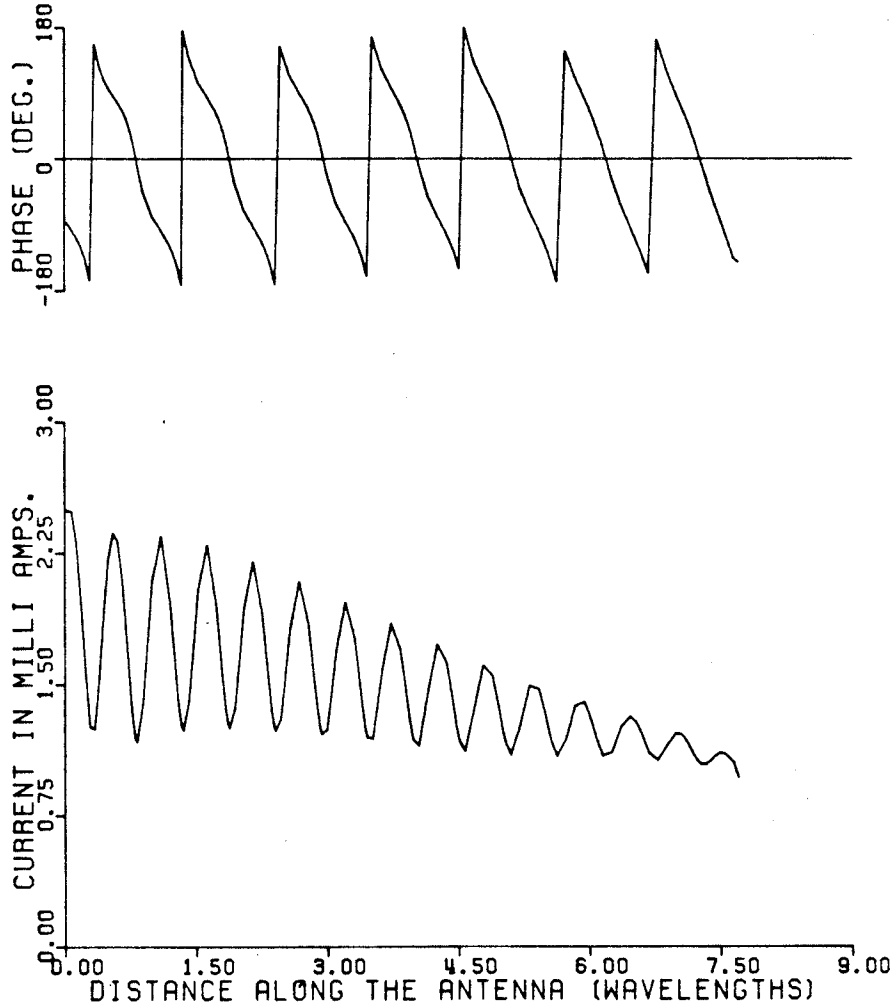

FIG. 2.12 PHASE AND CURRENT DISTRIBUTIONS ALONG THE UNDULATED WIRE

HEIGHT OF THE ELEMENT 0.10 WAVELENGTH

2.5 RESULTS AND DISCUSSION

In this chapter, a simplifying approximate expression for the array factor of sandwich wire antenna having a rectangular undulation was obtained. A comparison of the antenna patterns obtained using this approximate expression with the numerical solution using NEC, indicated that good agreement between the results of these two methods can be obtained, provided a proper attenuation constant is selected. The main difference between the patterns of the two methods was in the location of pattern nulls. This difference which is evident from Figures 2.13 to 2.14, was thought to be due to the variation of antenna resonant frequency with the undulation height. To examine this effect, Table 2.1 is included, which shows the phase variation per undulation as a function of undulation height. These results show that as the undulation height increases the phase progression reduces. Note that in all cases the physical length of each undulation was assumed to be one wavelength. It is clear that by increasing the undulation height the antenna element progressively looks shorter. Thus, in design of sandwich wire antennas, one must compensate for these phase reductions by increasing the element length.

Table 2.1 also shows that the phase progression along the array is not constant. This difference of phase per undulation along the array is due to the effect of the reflected wave, which could not be eliminated.

In summary, in this chapter the radiation from a sandwich wire antenna with rectangular undulation was studied using the uniform

point source array theory [30]. Comparing the results with the results of the NEC, which determines the array currents numerically, it was shown that the array theory can be used effectively to model the sandwich wire antenna. The comparison also showed that the antenna elements generally resonate at a frequency which is higher than the resonance frequency which is calculated using the physical lengths of the array. Although the array factor approach is an approximate one, it helps in understanding the radiation mechanism of the sandwich wire antenna.

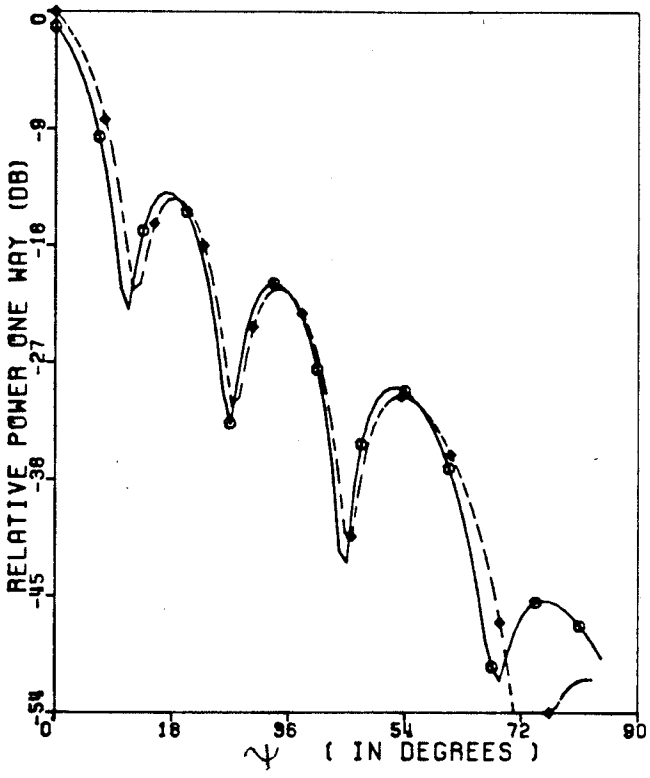

FIG. 2.13 RADIATION PATTERNS (END-FED)

◆ USING A.F EXPRESSION $\alpha = 0.3$

⊙ USING NEC HEIGHT OF THE ELEMENT = 0.16λ

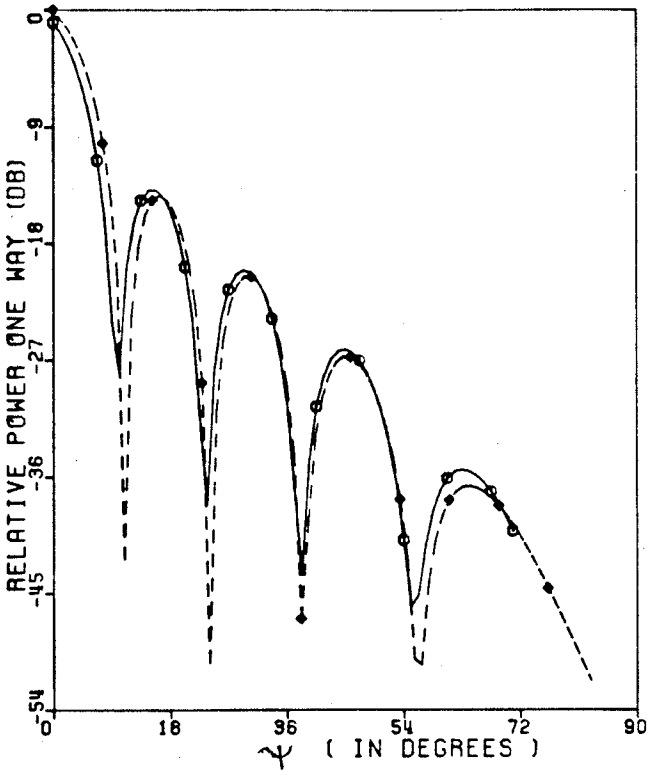

FIG. 2.14 RADIATION PATTERNS (END-FED)

◆ USING A.F EXPRESSION $\alpha = 0.22$

⊙ USING NEC HEIGHT OF THE ELEMENT = 0.10 λ

TABLE 2.1

PHASE VARIATION ALONG UNDULATED RECTANGULAR ANTENNA

UNDULATION NUMBER	HEIGHT OF THE UNDULATION IN WAVE LENGTH		
	0.1λ PHASE (DEG)	0.15λ PHASE (DEG)	0.2λ PHASE (DEG)
1	345.5	335.5	330.71
2	350	348.4	356.4
3	351.7	352.3	357.8
4	352	352.6	355.8
5	354.1	352.8	360.0
6	350.5	347.2	347.0

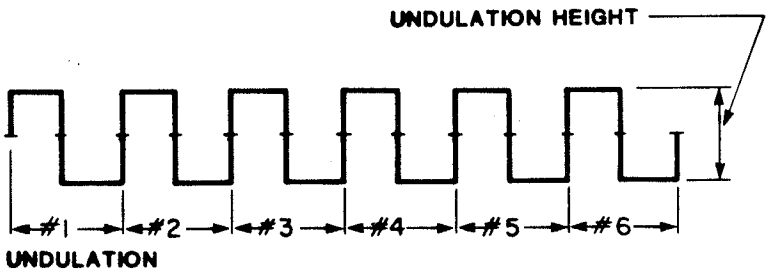

UNDULATED RECTANGULAR ANTENNA OF 6 UNDULATIONS

Chapter III

DESIGN OF SANDWICH WIRE ANTENNA

3.1 INTRODUCTION

In chapter 2 it was found that when the attenuation constant along the array is included in the array factor expression the sidelobe level can be reduced. In order to achieve lower sidelobe levels, it is necessary to vary the undulation height of the central conductor as a function of distance along the antenna length [8]. Rotman and Karas [1] reported a sandwich wire antenna of sinusoidal shape with a tapered undulation height. Their design did not give lower than -20 dB sidelobe levels and was an end-fed configuration. Graham and Dawson [6] developed a planar array with a number of sandwich antennas stacked together. The individual antennas were designed to produce a Taylor's aperture field amplitude distribution with a sidelobe level of -30 dB [6]. The measured sidelobe levels were about -26 dB. They claimed that the total reflections from the bends were cancelled out using a series of capacitive stubs placed transversely across the central conductor.

The design of sandwich wire antennas with very low sidelobe level is attempted in this chapter. The most important methods to achieve narrow main beams and low sidelobes are

1. Dolph - Chebyshev method for linear arrays [29]

2. Taylor Line source method [10].

In the present work the Taylor's line source method is used since it is more convenient to design non-uniformly spaced arrays.

3.2 THE TAYLOR LINE SOURCE METHOD

The antenna space factor for the Taylor distribution is given by [10]

$$F(z) = \frac{\sin(\pi z)}{\pi z} \frac{\prod_{n=1}^{\bar{n}-1} \left[1 - \left(\frac{\pi z}{z_n}\right)^2 \right]}{\prod_{n=1}^{\bar{n}-1} \left[1 - \left(\frac{z}{n}\right)^2 \right]} \qquad (3.1)$$

where

$$z_n = \pi \frac{\ell}{\lambda} \cos \Theta_n = \pm \pi \sigma \sqrt{A^2 + (n - 1/2)^2} \qquad 1 \leq n \leq \bar{n}$$

$$A = \frac{1}{\pi} \cosh^{-1}(\eta)$$

$$\sigma = \frac{\bar{n}}{\sqrt{A^2 + (\bar{n} - 1/2)^2}}$$

η is the sidelobe voltage ratio

Θ_n is the location of the nulls

z_n zeros of the Taylor pattern

The function F(z) in equation (3.1) becomes indeterminate for integer values of z. Using L'Hopital's rule it can be expressed as

$$F(z) = \pi \frac{\cos(\pi z)}{\pi z} \frac{\prod_{n=1}^{\bar{n}-1} \left[1 - \frac{z^2}{\sigma^2 \{A^2 + (n-1/2)^2\}} \right]}{\left[\frac{-2z}{n^2}\right]_{(z=n)} \prod_{n=1}^{\bar{n}-1} \left[1 - \frac{z^2}{n^2} \right]_{(n=z \text{ excluded})}}$$

$$F(z) = -\frac{\cos(\pi z)}{2} \frac{\prod_{n=1}^{\bar{n}-1}\left[1 - \frac{z^2}{\sigma^2\{A^2 + (n+1/2)^2\}}\right]}{\prod_{n=1}^{\bar{n}-1}\left[1 - \frac{z^2}{n^2}\right]_{(n=z \text{ excluded})}} \tag{3.2}$$

The amplitude distribution function g(p) of a line source is given by [10]

$$g(p) = \frac{1}{2\pi}\left[F(o) + 2\sum_{m=1}^{\bar{n}-1} F(m) \cdot \cos(mp)\right] \tag{3.3}$$

where

$$p = \pi x/a \qquad -a \le x \le a.$$

$$2a = \ell$$

ℓ is the length of the antenna.

The half-power beam width is given approximately by [29]

$$\Delta\omega = 2 \sin^{-1}\{\frac{\lambda}{\pi}\frac{\sigma}{\ell}(\cosh^{-1}\eta) - (\cosh^{-1}\frac{\eta}{\sqrt{2}})^2]^{1/2}\} \tag{3.4}$$

To initiate a Taylor design one should

1. specify the sidelobe level of the pattern
2. choose a positive integer value for $\bar{n}$, to insure the equality of the first sidelobes.

In this chapter, if the desired sidelobe level is assumed -40 dB, then A = 1.6864. Choosing $\bar{n} = 7, \sigma = 1.0424$, the normalized amplitude distribution along the array is calculated using the above equations and will then be used to compare the near field distribution.

3.3 ATTENUATION ALONG THE ANTENNA

The phase velocity and the attenuation constant of the sandwich wire antenna should be known in order to design the antenna. The attenuation constant along the array is expressed as a function of its amplitude distribution and is given by [2]

$$2\,\alpha\,(Z) = \frac{A^2(Z)}{\int_Z^L A^2(Z)dZ \;+\; \frac{P_L}{P_i - P_L}\int_o^L A^2(Z)dZ} \tag{3.5}$$

where

α = attenuation constant

Z = distance along the array

P_L = power dissipated in the load

P_i = power at the input

L = the total length of the antenna

$A(Z)$ = the aperture amplitude distribution

Equation 3.5 in the normalized form can be expressed as

$$\alpha\,(z) = \frac{0.5\,A^2(z)}{L\left(\frac{1}{1-b}\right)\int_o^1 A^2(z)\,dz \;-\; L\int_o^z A^2(z)\,dz} \tag{3.6}$$

where

$$z = \frac{Z}{L}$$

$$b = \frac{P_L}{P_i}$$

For a line-source antenna with the Taylor's amplitude distribution, A(z) in equation 3.6 should be calculated using equation 3.3. The attenuation constant of the antenna can therefore be calculated from equation 3.6.

3.4 DESIGN PROCEDURE

The geometry of a centre fed undulated line antenna is shown in Figure 3.1, where the undulation line has a rectangular geometry. It is assumed that most of the radiation is due to the vertical portions of the undulation (i.e. the sections along the y-axis in Fig. 3.1), which contribute to the current attenuation. On the horizontal portions, the current is assumed to remain constant and, thus, the horizontal portions do not contribute to its attenuation. To design such an antenna the following parameters are defined.

x_n = the position of n^{th} half-period along the x axis

H_n = the height of the n^{th} half-period

I_n = the current at the trailing end of the half-period

A_n = the amplitude ratio of the aperture fields at x_o and x_n

λ = the free space wavelength along the conductor

N = the total number of half-period sections

The design equations of the antenna are given by [9]

$$\lambda/2 = 2H_n + X_n - X_{n-1} \tag{3.7}$$

$$I_n = I_{n-1} \exp[-\alpha_{n-1}(H_{n-1} + H_n)] \tag{3.8}$$

$$A_n = \frac{I_n(H_n + H_{n+1})}{I_o H_1} \tag{3.9}$$

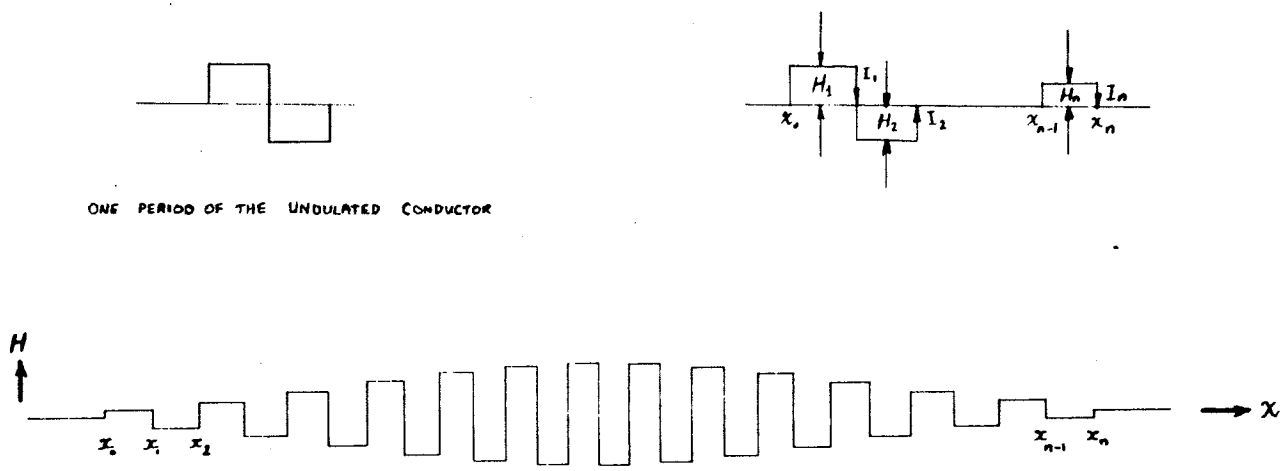

FIG. 3.1 GEOMETRY OF THE UNDULATED CONDUCTOR USING DESIGN EQUATIONS

TABLE 3.1

DIMENSION OF THE UNDULATED CONDUCTOR USING DESIGN EQUATION

n	H_n	$X_{n+1} - X_n$
1	0.0148705	0.4706192
2	-0.0212320	0.4575357
3	0.0292194	0.4415607
4	-0.0383628	0.4232740
5	0.0482005	0.4035988
6	-0.0581874	0.3836250
7	0.0677932	0.3644133
8	-0.0765727	0.3468542
9	0.0841972	0.3316050
10	-0.0913402	0.3190979
11	0.0952060	0.3095872
12	-0.0983986	0.3032027
13	0.1000000	0.3000000
14	-0.1000000	0.3000000
15	0.0983986	0.3032027
16	-0.0952060	0.3095872
17	0.0913402	0.3190979
18	-0.0841972	0.3316050
19	0.0765727	0.3468542
20	-0.0677932	0.3644133
21	0.0581874	0.3836250
22	-0.0482005	0.4035988
23	0.0383628	0.4232740
24	-0.0292194	0.4415607
25	0.0212320	0.4575357
26	-0.0148705	0.4706192

An initial value for H_1 is assumed and the value of x_n, I_n and H_{n+1} are determined from equation (3.7), (3.8), (3.9) respectively. Equation 3.7 is based on the fact that the total electrical length of each section of the undulation (each period) is equal to $\frac{\lambda}{2}$. The attenuation constant α_{n-1} in equation 3.8 can be calculated from equation 3.6 and the amplitude ratio of the aperture fields at X_o and X_n from equation 3.3. The height of the undulation should be less than $\frac{\lambda}{4}$ so that its total length can be retained at $\frac{\lambda}{2}$. The model which will be used in this design is an antenna with $b = 0.1$ (this model will be referred to as model #1). The values of X_n and H_n are calculated through a computer program and are listed in Table 3.1.

3.5 RADIATION CHARACTERISTICS OF THE CENTRE-FED SANDWICH WIRE ANTENNA

The design procedure developed in the previous section is an approximate one, since the mutual coupling between different radiating sections of the antenna are not included. It is therefore desirable to investigate its near field and far field radiation characteristics to examine the validity of the design procedure. To undertake this study, the geometry of the antenna of model #1 is used as input to the Numerical Electromagnetic Code and its radiation patterns are computed in the frequency range of 300 MHz to 355 MHz. The results are shown in Figures 3.2a to 3.5a.

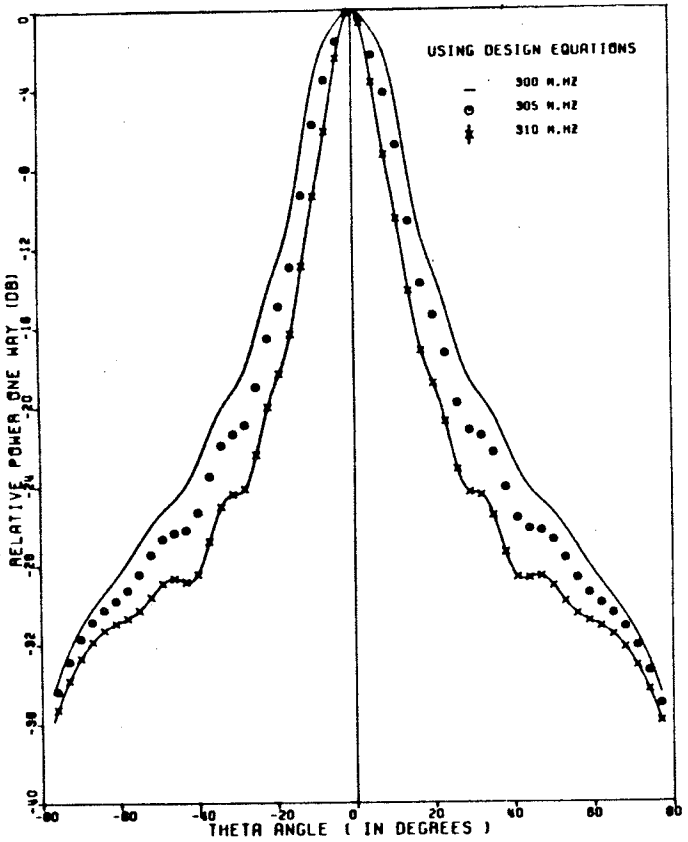

FIG. 3.2 a H-PLANE RADIATION PATTERN OF A CENTRE-FED TAPERED SANDWICH WIRE ANTENNA AT DIFFERENT FREQUENCIES

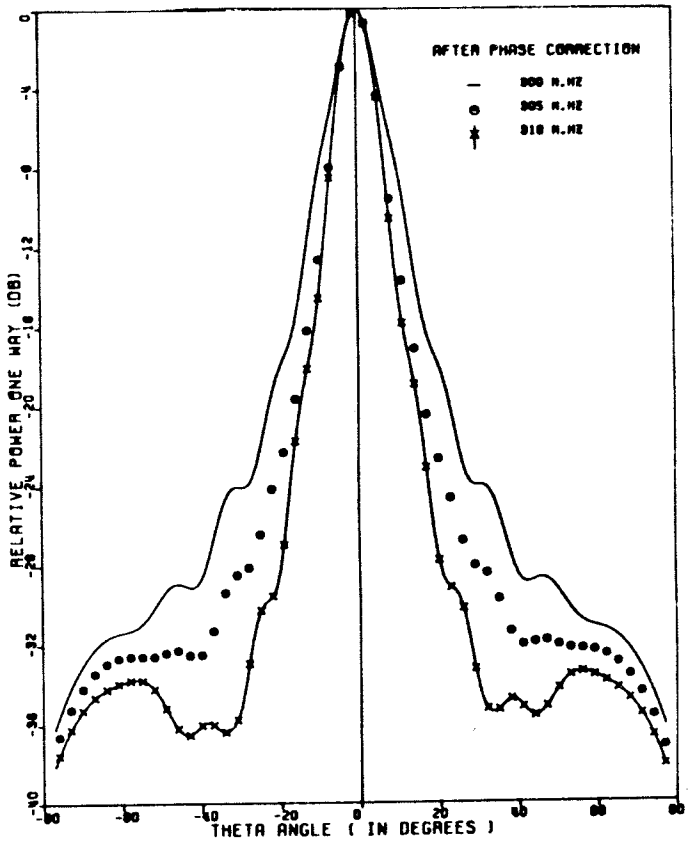

FIG. 3.2 b H-PLANE RADIATION PATTERN OF A CENTRE-FED TAPERED SANDWICH WIRE ANTENNA AT DIFFERENT FREQUENCIES

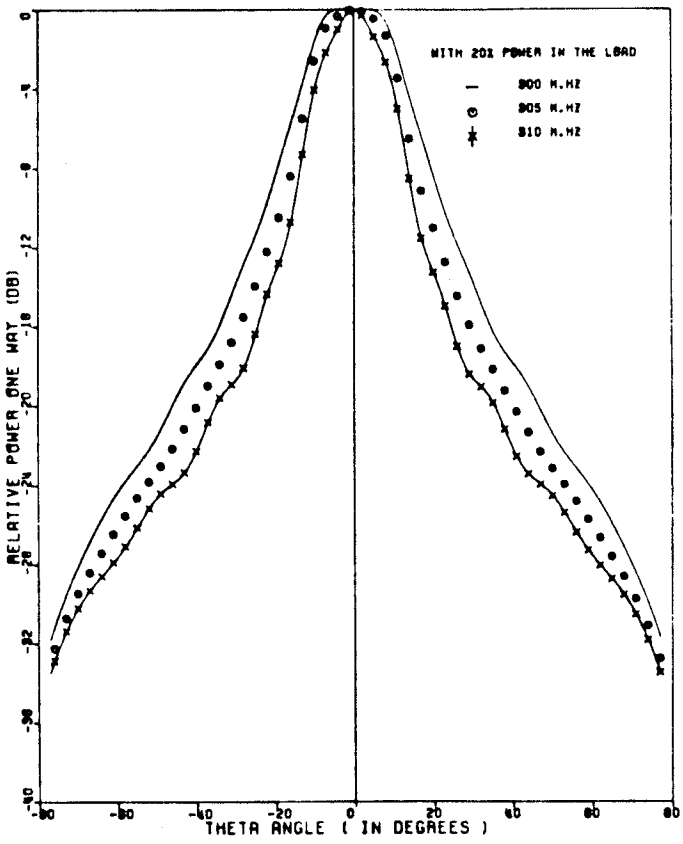

FIG. 3.2c H-PLANE RADIATION PATTERN OF A CENTRE-FED TAPERED SANDWICH WIRE ANTENNA AT DIFFERENT FREQUENCIES

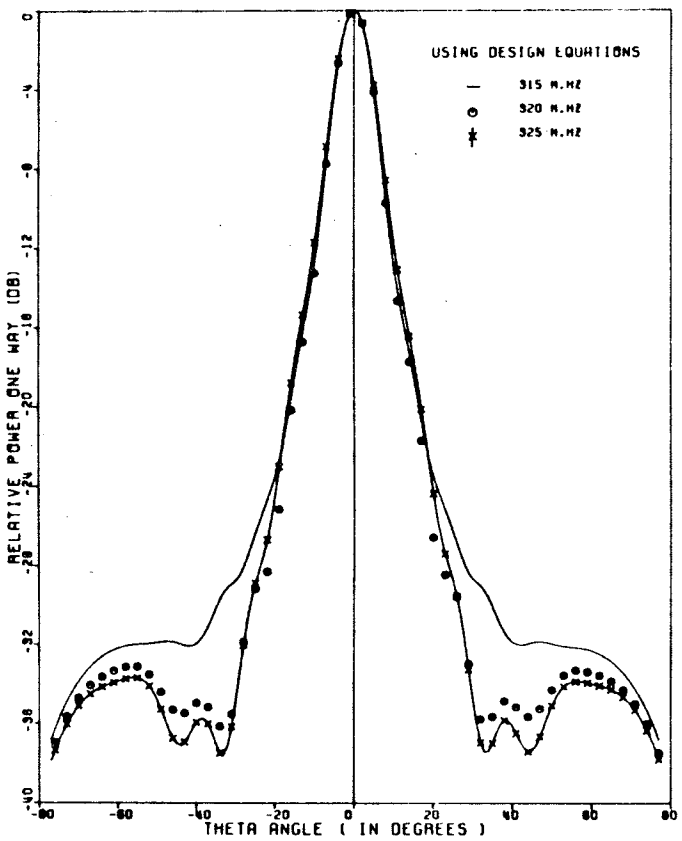

FIG. 3.3a H-PLANE RADIATION PATTERN OF A CENTRE-FED TAPERED SANDWICH WIRE ANTENNA AT DIFFERENT FREQUENCIES

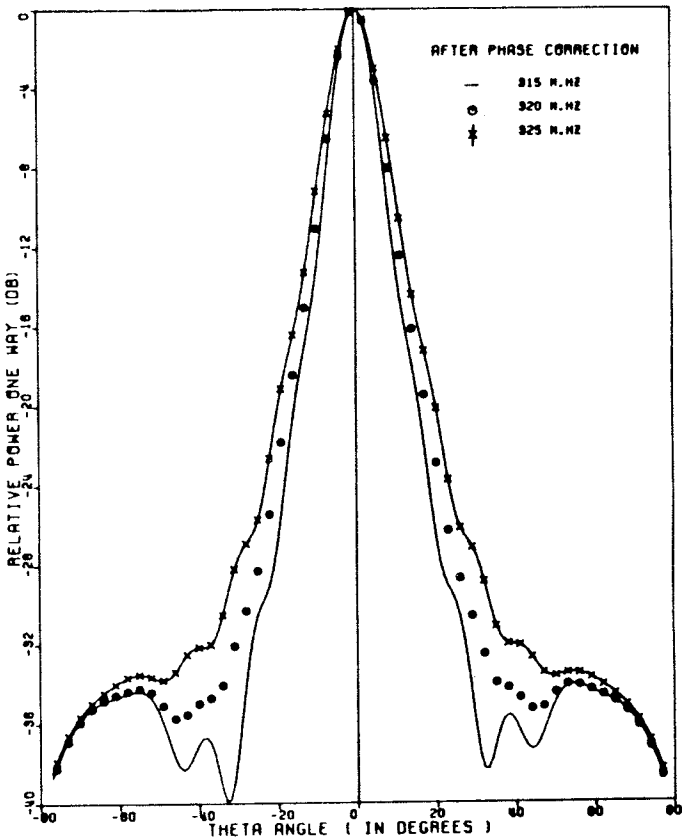

FIG. 3.3b H-PLANE RADIATION PATTERN OF A CENTRE-FED TAPERED SANDWICH WIRE ANTENNA AT DIFFERENT FREQUENCIES

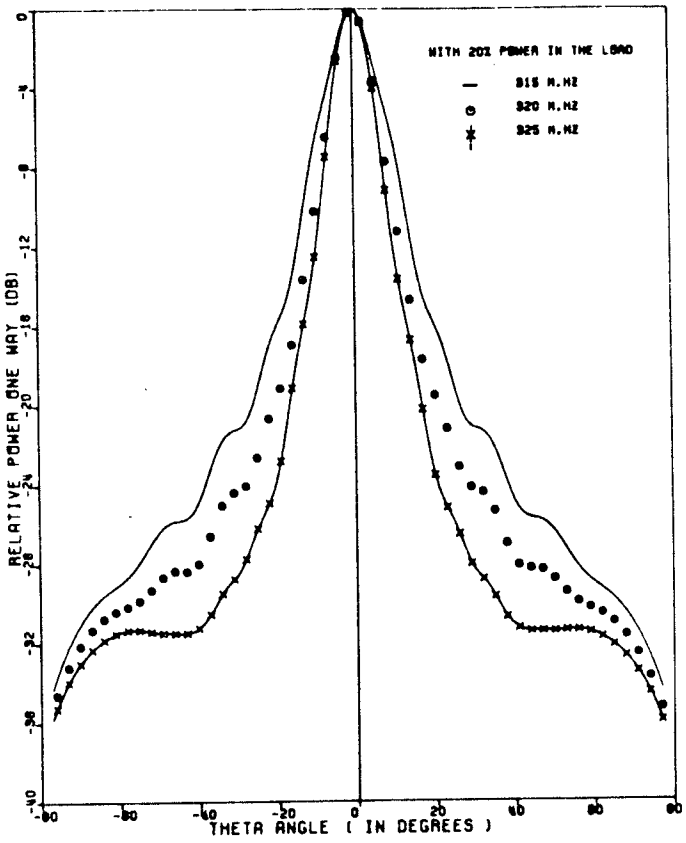

FIG. 3.3 c H-PLANE RADIATION PATTERN OF A CENTRE-FED TAPERED SANDWICH WIRE ANTENNA AT DIFFERENT FREQUENCIES

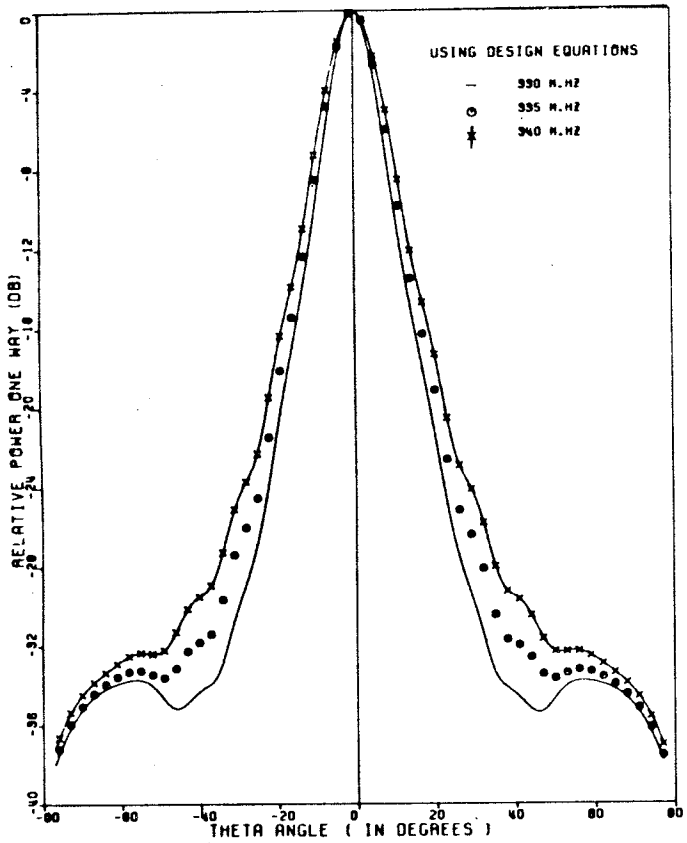

FIG. 3.4a H-PLANE RADIATION PATTERN OF A CENTRE-FED TAPERED SANDWICH WIRE ANTENNA AT DIFFERENT FREQUENCIES

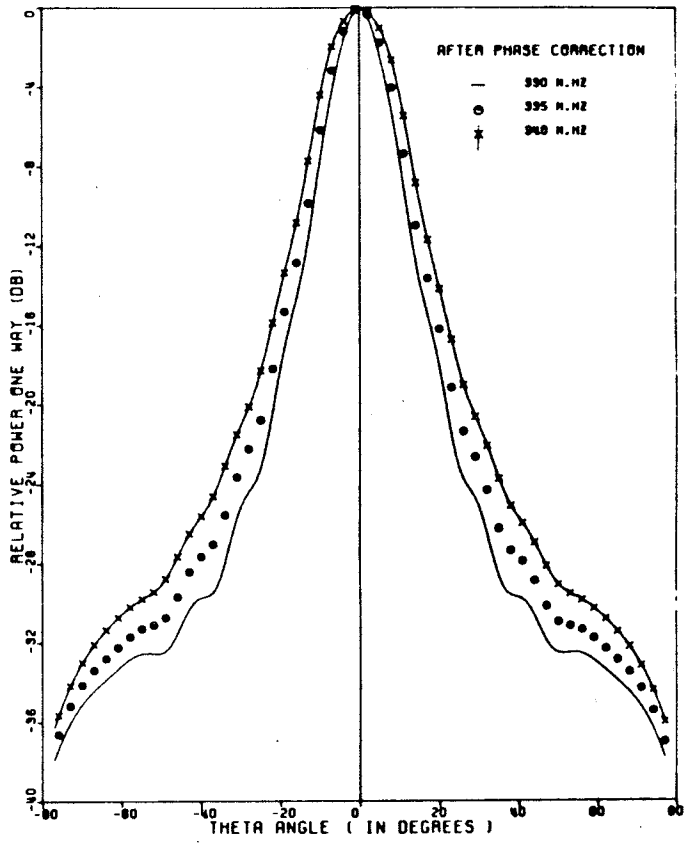

FIG. 3.4b H-PLANE RADIATION PATTERN OF A CENTRE-FED TAPERED SANDWICH WIRE ANTENNA AT DIFFERENT FREQUENCIES

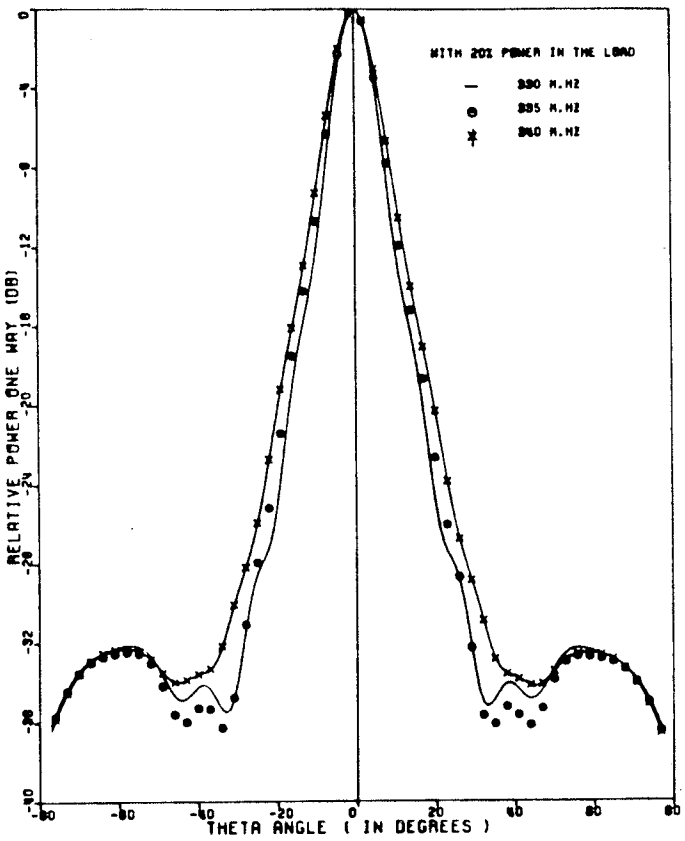

FIG. 3.4c H-PLANE RADIATION PATTERN OF A CENTRE-FED TAPERED SANDWICH WIRE ANTENNA AT DIFFERENT FREQUENCIES

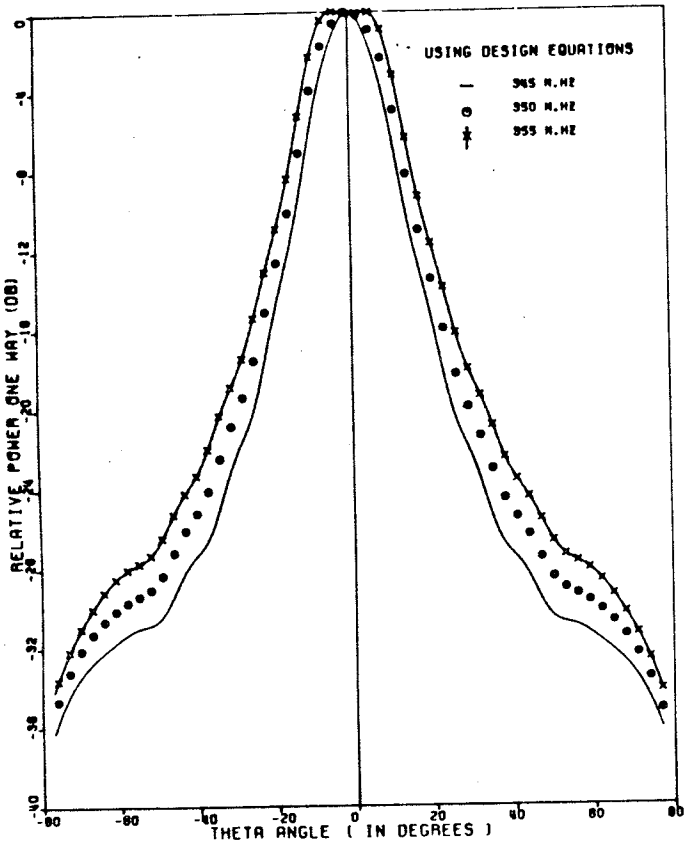

FIG. 3.5a H-PLANE RADIATION PATTERN OF A CENTRE-FED TAPERED SANDWICH WIRE ANTENNA AT DIFFERENT FREQUENCIES

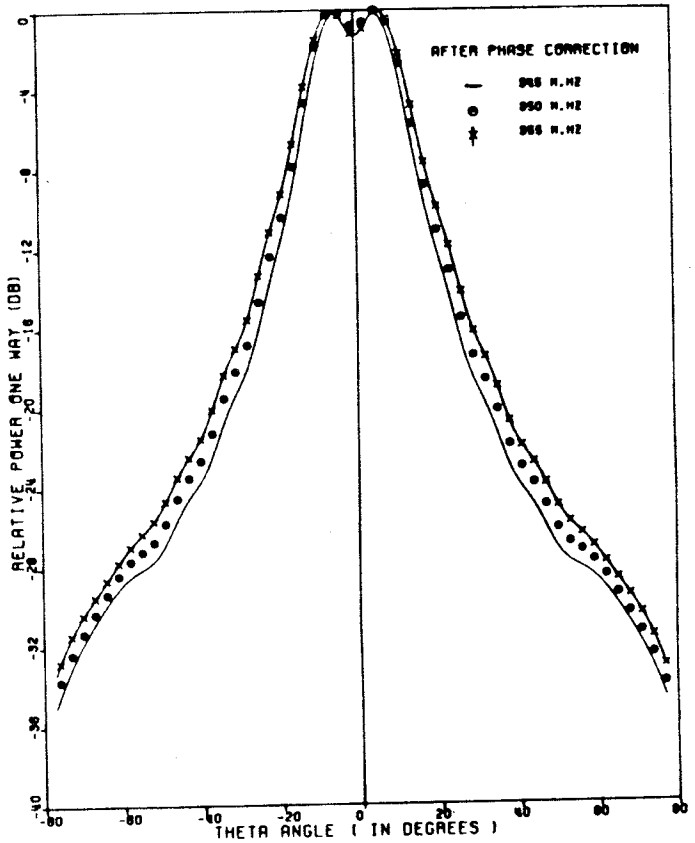

FIG. 3.5b H-PLANE RADIATION PATTERN OF A CENTRE-FED TAPERED SANDWICH WIRE ANTENNA AT DIFFERENT FREQUENCIES

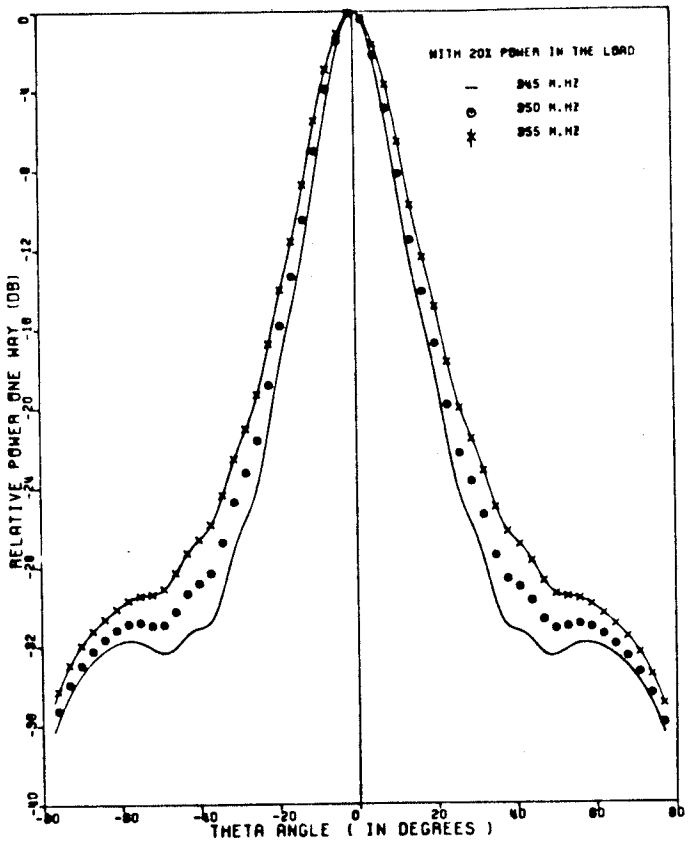

FIG. 3.5c H-PLANE RADIATION PATTERN OF A CENTRE-FED TAPERED SANDWICH WIRE ANTENNA AT DIFFERENT FREQUENCIES

An examination of these figures indicates that the radiation patterns of the antenna are frequency dependent and generally have higher sidelobe levels than -40 dB, the design goal. The best radiation pattern is at 325 MHz, which gives the narrowest beam width and the lowest sidelobe level of about -34 dB. The first sidelobe level, at this frequency, is about -36 dB. By increasing or decreasing the frequency, the radiation patterns gradually broaden and the peak sidelobe levels increase. However, both beam widths and sidelobe levels seem relatively constant for a 6 percent bandwidth from 320 MHz to 340 MHz.

The above antenna was designed without a modification of the antenna element, to correct the phase reduction due to the corners. To examine the possibility of improving the antenna performance by incorporating the phase correction, the antenna of model #2 was designed. This antenna is the same as model #1, but the element lengths, X_n, are increased according to the data of Table 2.1. Its radiation patterns are presented in Figures 3.2(b) to 3.5(b). Comparing these results with those of model #1, one notes that the performance of this antenna is similar to model #1, but its centre frequency has shifted from 325 MHz to around 310 MHz. The dimensions of this model (model #2) are listed in Table 3.2.

The near field distributions of both above antennas are also computed and are shown in Figures 3.6 and 3.7, respectively. Their near field distributions are similar, but somewhat different than the assumed Taylor distribution. An examination of

TABLE 3.2

DIMENSION OF THE UNDULATED CONDUCTOR AFTER PHASE CORRECTION

n	H_n	$X_{n+1} - X_n$
1	0.0148705	0.4568192
2	-0.0212320	0.4437357
3	0.0292194	0.4277607
4	-0.0383628	0.4094740
5	0.0482005	0.3897988
6	-0.0581874	0.3698250
7	0.0677932	0.3506132
8	-0.0765727	0.3330542
9	0.0841972	0.3178049
10	-0.0913402	0.3052979
11	0.0952060	0.2957872
12	-0.0983986	0.2894027
13	0.1000000	0.2861999
14	-0.1000000	0.2861999
15	0.0983986	0.2894027
16	-0.0952060	0.2957872
17	0.0913402	0.3052979
18	-0.0841972	0.3178049
19	0.0765727	0.3330542
20	-0.0677932	0.3506132
21	0.0581874	0.3698250
22	-0.0482005	0.3897988
23	0.0383628	0.4094740
24	-0.0292194	0.4277607
25	0.0212320	0.4437357
26	-0.0148705	0.4568192

these figures shows that the antenna elements toward the end radiate less energy than the required Taylor distribution. This deviation of the antenna near fields from the required Taylor distribution is a possible cause of the higher sidelobe levels. In practice, if an antenna with a lower sidelobe level is required, it may be designed by an iteration process to improve the antenna near field distribution.

As a final check, the variable b which is the percentage of the antenna power delivered to the load, is also modified to examine its effect on the design. Selecting b=0.2 a new antenna was designed and studied. The dimensions of this antenna are listed in Table 3.3. Its radiation patterns are shown in Figures 3.2c to 3.5c and its near field is shown in Figure 3.8. For this design, the radiation patterns have higher sidelobe levels, indicating that increasing the parameter b does not improve the antenna radiation patterns. This poor performance is due to further deviation of its near field distribution from the required Taylor distribution.

TABLE 3.3

DIMENSION OF THE UNDULATED CONDUCTOR WITH 20 % POWER IN THE LOAD

n	H_n	$X_{n+1} - X_n$
1	0.0149301	0.4563395
2	-0.0200472	0.4461056
3	0.0292443	0.4277111
4	-0.0368800	0.4124399
5	0.0480750	0.3900496
6	-0.0564683	0.3732630
7	0.0676350	0.3509299
8	-0.0747078	0.3367840
9	0.0840921	0.3180157
10	-0.0885068	0.3091851
11	0.0951717	0.2958560
12	-0.0964146	0.2933707
13	0.1000000	0.2861999
14	-0.1000000	0.2861999
15	0.0964146	0.2933707
16	-0.0951717	0.2958560
17	0.0885068	0.3091851
18	-0.0840921	0.3180157
19	0.0747078	0.3367840
20	-0.0676350	0.3509299
21	0.0564683	0.3732630
22	-0.0480750	0.3900496
23	0.0368800	0.4124399
24	-0.0292443	0.4277111
25	0.0200472	0.4461056
26	-0.0149301	0.4563395

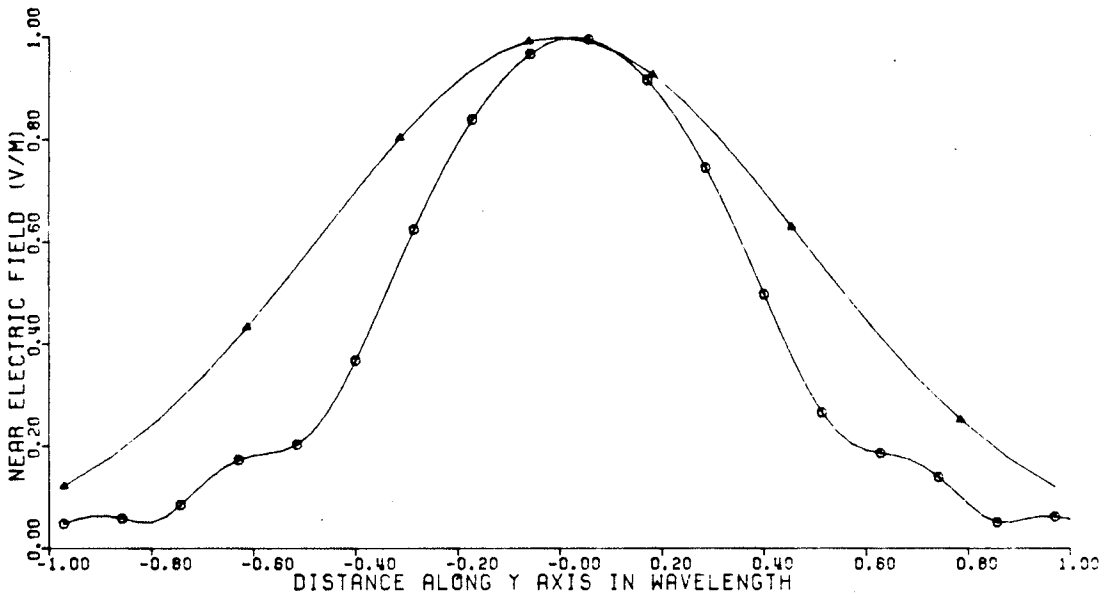

FIG. 3.6 NEAR FIELD DISTRIBUTION

▲ THEORETICAL TAYLOR

⊙ DUE TO MODEL #1 AT FREQUENCY 325 M.HZ.

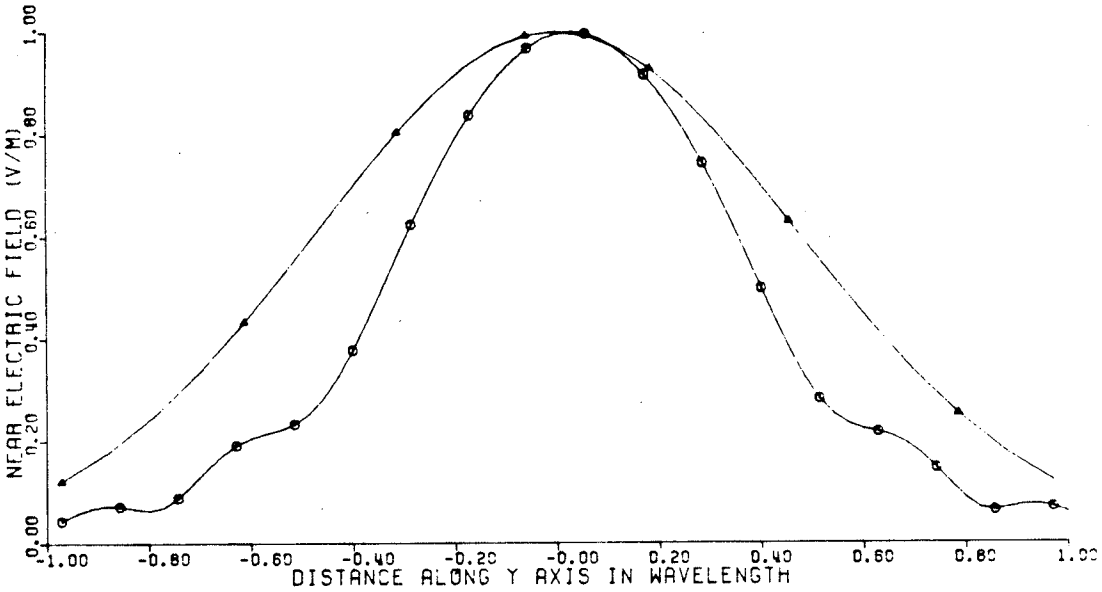

FIG. 3.7 NEAR FIELD DISTRIBUTION

▲ THEORETICAL TAYLOR

⊙ DUE TO MODEL •2 AT FREQUENCY 315 M.HZ.

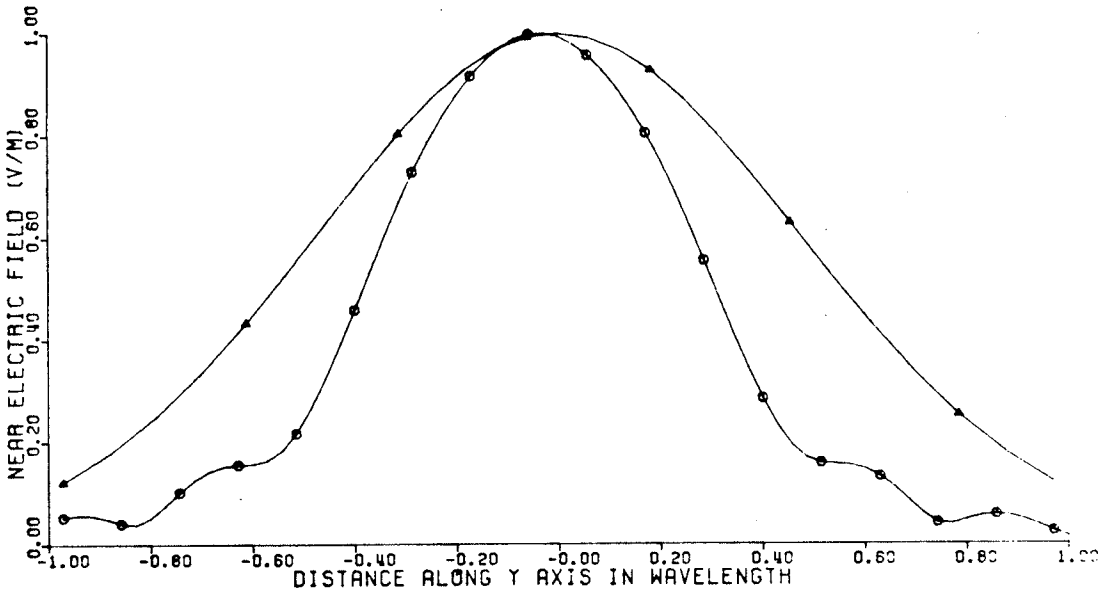

FIG. 3.8 NEAR FIELD DISTRIBUTION

▲ THEORETICAL TAYLOR

⊙ 20 % POWER IN THE LOAD AT FREQUENCY 315 MHZ.

3.6 RESULTS AND DISCUSSION

In this chapter approximate design equations for the tapered rectangular sandwich wire antenna were obtained. These design equations were based on the Taylor line source method [10]. The geometry of the antenna, obtained by using these equations, was used as input data to the Numerical Electromagnetic Code which computed the radiation patterns at different frequencies. The antenna was designed for sidelobe levels of -40 dB, but the results obtained show that the radiation patterns have sidelobe levels higher than -40 dB. The deviation in the sidelobe level from the desired value was thought to be due to the phase error along the array. However, when the phase along the array was corrected, the performance of the antenna remains the same as the previous case but its centre frequency shifted from 325 MHz to 310 MHz. The near field distributions for both cases were similar but somewhat different from the assumed Taylor distribution. By examining the effect of the power delivered to the load, it was found that by increasing the load power, the sidelobe level increased and the near field distribution deviated further from the Taylor distribution.

The results presented in this chapter indicated that sandwich wire antennas can be designed to provide radiation patterns with low sidelobe levels. However, the design procedure developed in this chapter neglected the mutual interaction between the radiating parts of the antenna. As a result, the computed sidelobes of the designed antennas were somewhat higher than the design

goal. Nevertheless, they provided sidelobes much lower than those of previously designed antennas.

Chapter IV

CALCULATION OF THE LINE IMPEDANCE

4.1 INTRODUCTION

Generally, the central undulated line is connected to both the generator and the load through a straight section of the line. It is therefore desirable to determine the impedance of a straight conductor inside a trough, so that the undulated line can be connected to the required circuit elements. Because the conductor is supported by dielectric substrate the problem will be treated as a suspended microstrip inside a trough. This chapter is concerned with the determination of the characteristic impedance and the relative wave velocity of a microstrip line in a trough. To simplify the problem, the mode of propagation in the microstrip is assumed to be transverse electromagnetic (TEM) wave, i.e., neither the electric nor the magnetic fields have components in the direction of propagation. Thus, the determination of the impedance and relative wave velocity requires a study of the fields only over the line cross-section. For such a case, it is known that the potential function obeys Laplace's equation [12] which must be solved subject to the imposed boundary conditions.

4.2 THEORETICAL PROCEDURE

The microstrip structure considered in the analysis is shown in Fig. 4.1. Assuming that the cross-section of the structure is defined by the boundaries 1 and 2 in Fig. 4.2, the potential function $\phi(x,y)$ can be obtained by solving Laplace's equation for the domain defined by the boundaries 1 and 2, and the surface at infinity. The function must satisfy the two-dimensional Laplace's equation,

$$\frac{\partial^2\phi}{\partial x^2} + \frac{\partial^2\phi}{\partial y^2} = 0 \tag{4.1}$$

with the following boundary conditions

$$\phi(x,y) = \phi_1 = 1 \tag{4.2}$$

$$\phi(x,y) = \phi_o = 0 \tag{4.3}$$

where

ϕ_1 is the potential on the strip (boundary 1).

ϕ_o is the potential on the walls (boundary 2).

Additional boundary conditions on $\phi(x,y)$ are also imposed, by assuming that it approaches zero at large distances from the object.

Once the distributed electrostatic potential is found, the electric field values can be determined. From these results one can determine the surface charge distribution and hence the capacitance of the line per unit length. The latter can be used to calculate the characteristic impedance of the line and its relative wave velocity [16,17]. In this thesis a finite difference technique is used to solve the Laplace's equation.

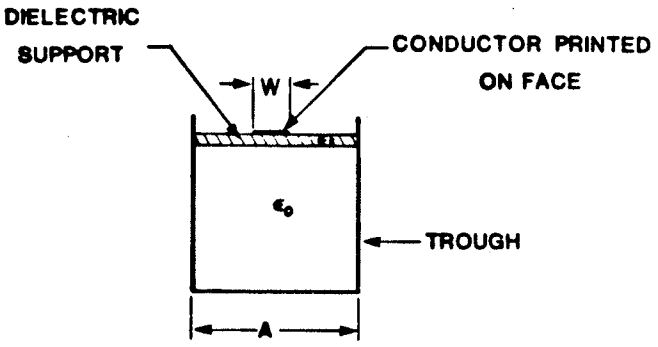

FIG.4.1 CROSS-SECTION OF SUSPENDED MICROSTRIP INSIDE A TROUGH

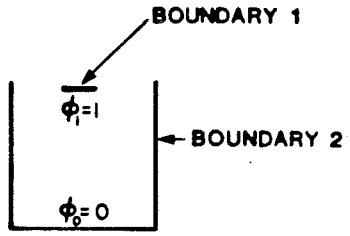

FIG.4.2 CROSS-SECTION OF STRIP LINE INSIDE A TROUGH

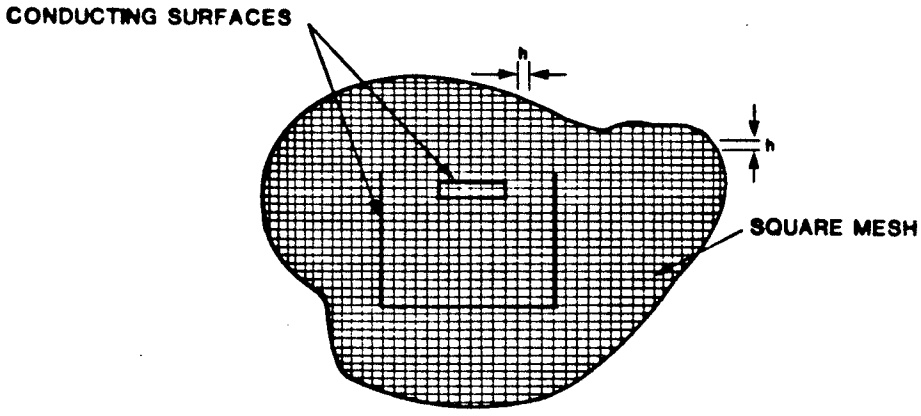

FIG.4.3 (a) BASIC FINITE DIFFERENCE MESH

4.3 FINITE DIFFERENCE REPRESENTATION

Considering the two-dimensional problem shown in Fig. 4.3(a), the region between the strip and the walls may be divided into square sub-areas, by a mesh of interlaced rows and columns. Fig. 4.3(a) shows the orientation of the conductors along these rows and columns, which is for the purpose of organizing the problem in the computer. Considering a typical point $\phi\ (x_i, y_i)$ in the medium between the strip and the walls, the potential at this point must satisfy equation (4.1). This equation ,using a finite difference approximation, can be expressed in a form which is suitable for numerical computation [19-21], and given by

$$\nabla^2\phi_{i,j} = \frac{1}{h^2}\left[\phi_{i+1,j} + \phi_{i-1,j} + \phi_{i,j+1} + \phi_{i,j-1} - 4\phi_{i,j}\right] = 0 \qquad (4.4)$$

The most common method for solving this equation is the successive over relaxation (S.O.R) [19-21], and the potential at the point of interest can be written as,

$$\phi_{i,j}^{(k+1)} = \phi_{i,j}^{(k)} + \frac{\phi_{i+1,j}^{(k)} + \phi_{i-1,j}^{(k)} + \phi_{i,j-1}^{(k)} + \phi_{i,j+1}^{(k)} - 4\phi_{i,j}^{(k)}}{4} \qquad (4.5)$$

To get faster convergence equation 4.5 can be rewritten as,

$$\phi_{i,j}^{(k+1)} = \phi_{i,j}^{(k)} + \omega_o \left[\frac{\phi_{i+1,j}^{(k)} + \phi_{i-1,j}^{(k)} + \phi_{i,j+1}^{(k)} + \phi_{i,j-1}^{(k)} - 4\,\phi_{i,j}^{(k)}}{4} \right] \qquad (4.6)$$

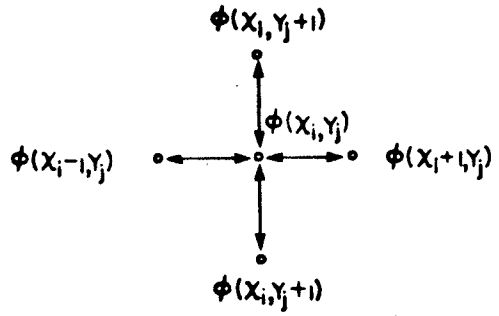

FIG.4.3 (b) MESH REPRESENTATION FOR POTENTIAL FOR ADJACENT MESH POINTS

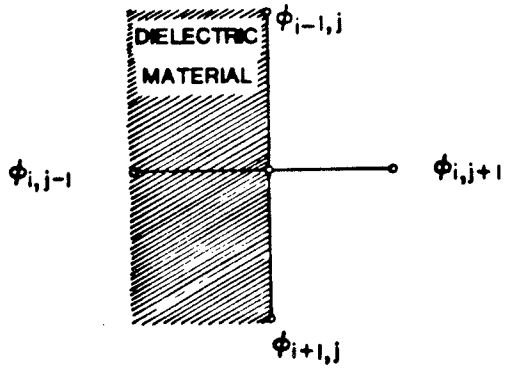

FIG.4.4 MESH POINTS ON DIELECTRIC BOUNDARY

where ω_o is the acceleration factor, and will always be between 1.0 and 2.0. ω_o is not always predictable in advance, but this difficulty was overcome by Carre [22].

4.3.1 Nodal Potential with Dielectric Support

In a practical design of a stripline shown in Fig. 4.1, it is necessary to support the stripline inside the trough. This can be accomplished by a dielectric substrate. In this case, equation (4.6) still holds, except for mesh points located on the interface of the two regions (i.e, air and dielectric) The difference equation for these points can be shown to be [16]

$$\phi_{i,j} = \frac{\phi_{i,j} + \varepsilon_r \phi_{i,j-1}}{2(1+\epsilon_r)} + \frac{\phi_{i-1,j} + \phi_{i+1,j}}{4} \qquad (4.7)$$

with the notation shown in Fig. 4.4. Equation 4.6 and 4.7 can be used to compute the required potential distributions. These computed potentials enable one to determine other field quantities that are essential for computation of the line impedance and the wave velocity. The steps leading to these computations are indicated in the following sections.

4.4 DETERMINATION OF THE IMPEDANCE AND RELATIVE VELOCITY

Having calculated the potentials on the nodal points of the mesh established in section (4.3), it is necessary to determine the charge on the strip by the Gauss's theorem [23] in order to obtain the capacitance. This requires the integration of the normal component of the electric flux density over a surface, which encloses the strip. This surface is formed by lines joining nodal points drawn parallel to the coordinate direction, as shown in Fig. 4.5. The electric flux density at any point on this surface is given by

$$D_n = -\epsilon \frac{\partial \phi}{\partial n} \tag{4.8}$$

where,

n is the unit vector normal to the surface

D_n is the normal component of electric flux density

Thus if the surface containing the conductor consists of 'ℓ' straight line segments each containing 'n' nodes, the charge per unit length normal to the cross-section is given by,

$$Q = \epsilon h \sum_{\ell}' \sum_{p=1}^{n}{}' \left(\frac{\partial \phi}{\partial n} \right)_p \tag{4.9}$$

where p is any point on the surface. The symbol $\sum'$ is used to indicate that the first and last terms in the summation are halved, which is equivalent to integration by the trapezoidal rule. From equation (4.9), the charge Q can be used to determine the capacitance c, the capacitance c is given by,

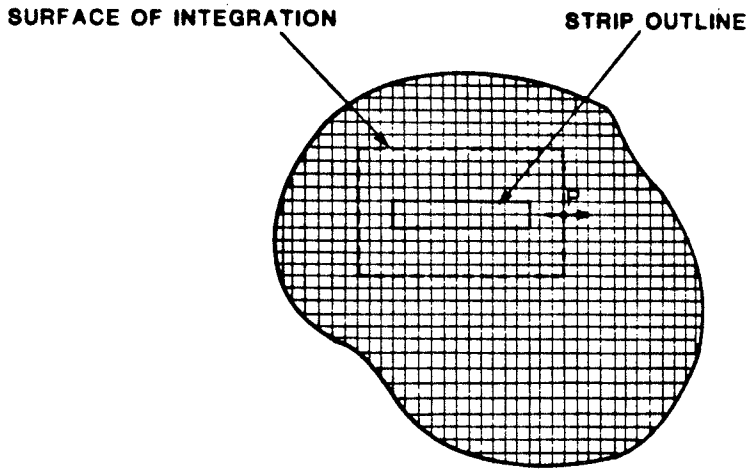

FIG.4.5 INTEGRATION TO DETERMINE THE CHARGE

$$c = \frac{Q}{\phi_\tau} \tag{4.10}$$

where ϕ_τ is the potential difference between the strip and the walls. If the region is homogeneous, that is, without dielectric, the characteristic impedance [24-27] is given by,

$$z_o = \frac{1}{cv} \tag{4.11}$$

$$v = v_o/\sqrt{\varepsilon_r}$$

where,

v is the phase velocity in the medium.

v_o is the phase velocity in free space.

ε_r is the dielectric constant of the medium.

If the medium is inhomogeneous, (i.e, contains dielectric materials) the characteristic impedance is then given by,[24]

$$z_o = \frac{1}{v_o\sqrt{cc_o}} \tag{4.12}$$

where

c_o is the capacitance without dielectric,

c is the capacitance with dielectric present,

The relative wave velocity is given by

$$v_r = \sqrt{\frac{c_o}{c}} \tag{4.13}$$

4.5 RESULTS AND DISCUSSION

A numerical analysis of the suspended microstrip in a trough as shown in Fig. 4.1, has been carried out using a computer program written for the finite difference method [18-19]. The region between the strip and the walls was divided into square subareas, by a mesh of interlaced rows and columns. The potential at every intersection was found by the successive over relaxation (S.O.R) method, and the iterative process terminated when the relative displacement norm $|\delta|/|\phi|$ is smaller than 0.001 . The displacement vector at the k^{th} iteration, $\delta^{(k)}$ is given by,

$$\delta^{(k)} = \phi^{(k)} - \phi^{(k-1)}$$

and the norm is defined by,

$$\| \delta \| = \sum_i |\delta_i|$$

The numerical accuracy of the computed results and the computer execution time depend on the number of node points per row or column, and the acceleration factor, ω_o . The number of mesh intervals along X and Y-axes were taken as 80, i.e., 79x79 interior points. The stripline was divided into 10 intervals. The optimum value of ω_o was found to be 1.7 and the number of iterations was found to be equal to 37. Table 4.1 shows the required number of iterations to achieve the convergence for ω_o from 1.1 to 1.9 . The optimum computer execution time was found to be 13 seconds, with ω_o=1.7. For special cases, the results were compared with these of Green [24,25] and Schneider [16], and the agreement for

the impedance within 4 percent limit was obtained. The characteristic impedances and the relative wave velocities for different substrate and line parameters are shown in Figs. 4.6-4.9. Fig. 4.6 shows the variation of the line impedance and the relative wave velocity as a function of line separation from the central axis. The thickness of the dielectric was taken as 1.59 mm. For a centrally located line, the variation of the characteristic impedance with the line width is shown in Fig. 4.7, for substrate of relative permittivity ε_r=2.32 and ε_r=4. The results of this figure can be used to select line widths for matching the line to a given load or to a given generator impedance. The variations of the relative wave velocity with the strip width and for ε_r=2.3 and ε_r=4.0 are shown in Fig. 4.8. Fig 4.9 shows the variation of the line characteristic impedance and the relative wave velocity with the microstrip width of 2 mm. thickness.

From all these figures, a decrease of the line impedance occurs if the ratio W/A or the dielectric constant or dielectric height is increased. This behaviour is expected since the structure resembles a parallel plate capacitor. Thus, by changing these parameters or the center offset distance, the desired value of the line characteristic impedance or relative wave velocity can be obtained. The results obtained in this chapter were compared with published theoretical and experimental results [14]. From this comparison it is found that the method outlined provides sufficiently accurate results. The results obtained can serve as useful data for design of the input and output terminations of sandwich wire antennas.

TABLE 4.1

EFFECT OF THE ACCELERATION FACTOR ON THE NUMBER OF ITERATION

ω_o	n
1.1	95
1.2	76
1.3	57
1.4	49
1.5	45
1.6	40
1.7	37
1.8	44
1.9	81

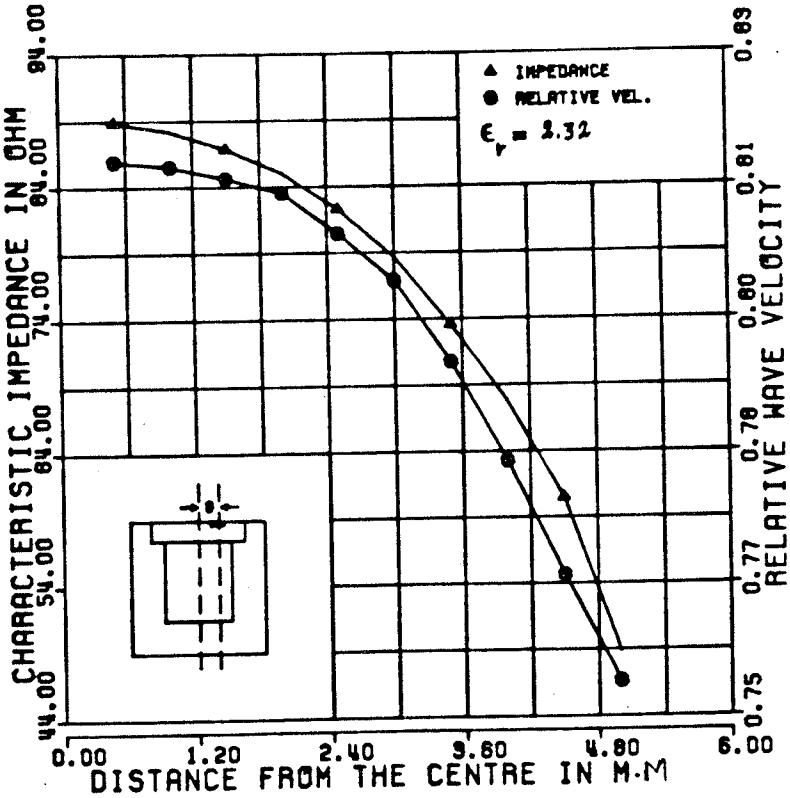

FIGURE 4.6 VARIATION OF LINE IMPEDANCE AND RELATIVE WAVE VELOCITY WITH CENTER OFFSET "S"

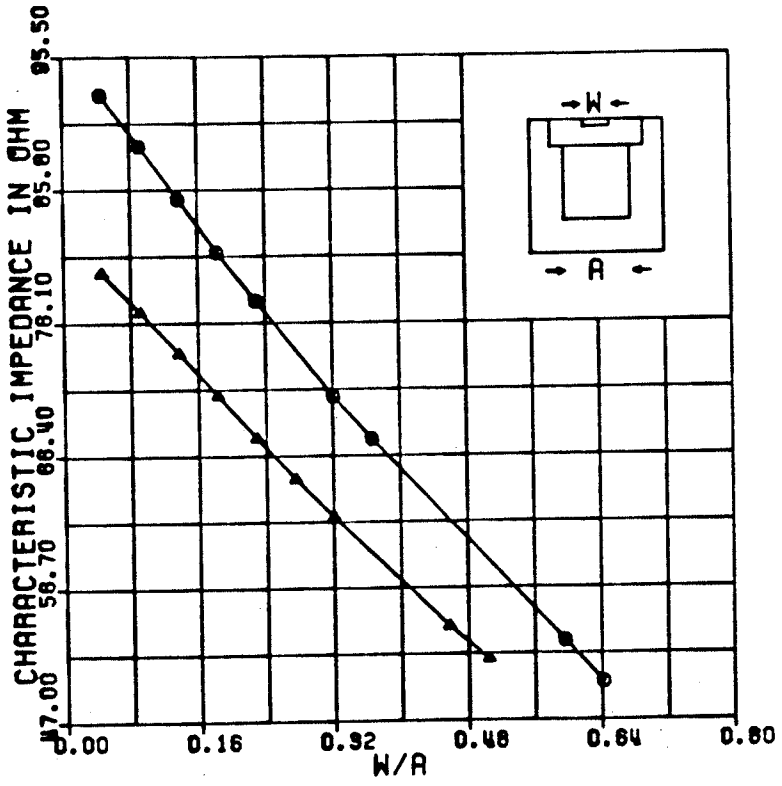

FIGURE 4.7 VARIATION OF THE LINE IMPEDANCE WITH STRIP WIDTH

○ ——— ϵ_r=2.32

▲ ——— ϵ_r=4.00

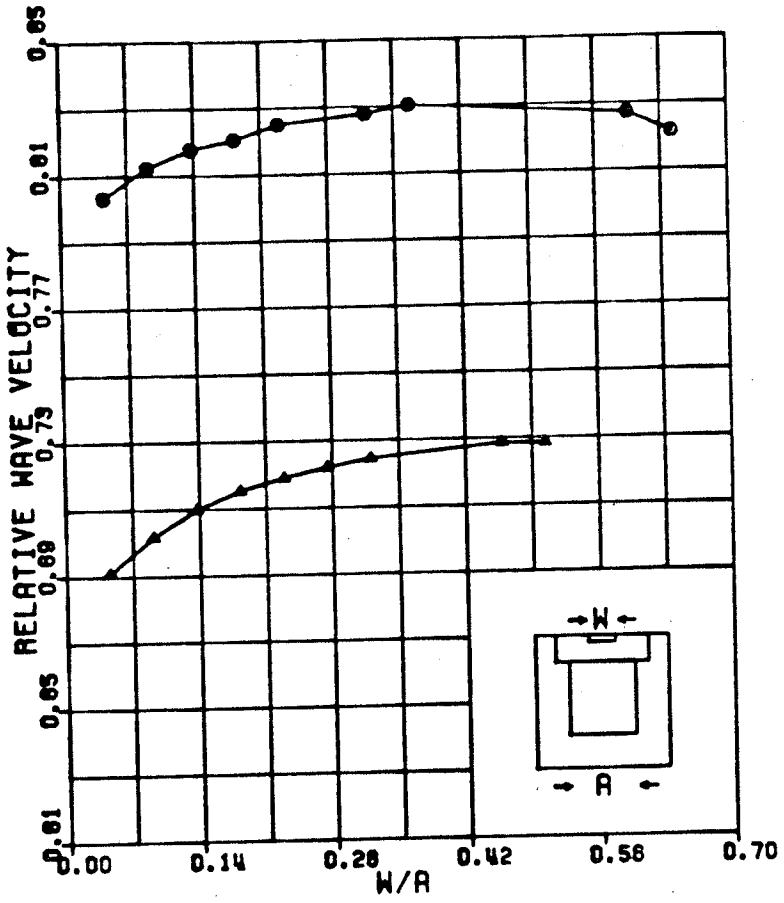

FIGURE 4.8 VARIATION OF THE RELATIVE WAVE VELOCITY WITH STRIP WIDTH

○ ——— ϵ_r=2.32

▲ ——— ϵ_r=4.00

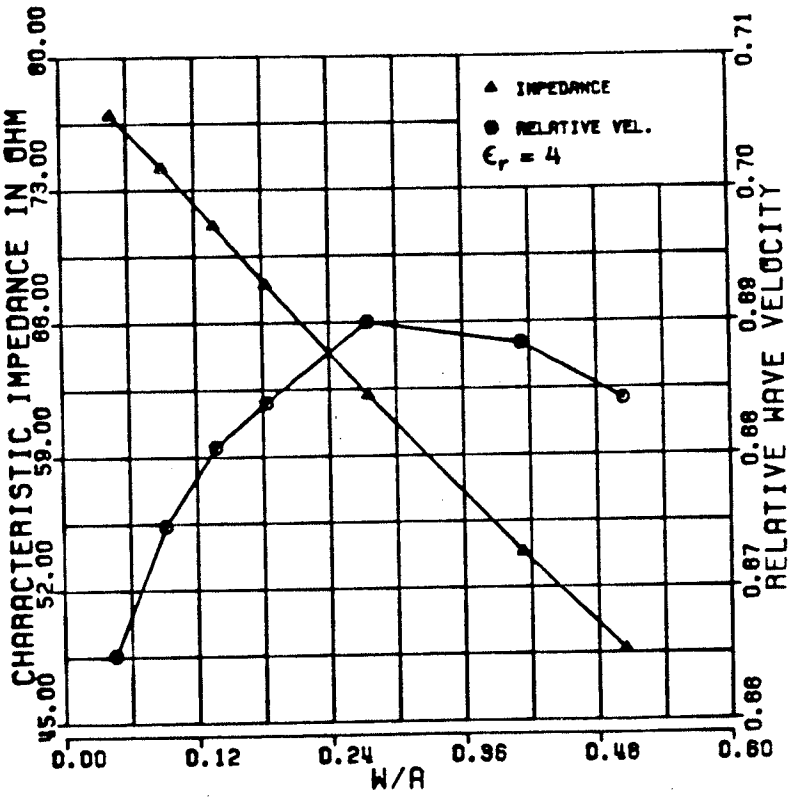

FIGURE 4.9 VARIATION OF THE IMPEDANCE AND RELATIVE WAVE VELCITY WITH DIELECTRIC THICKNESS =2 MM.

Chapter V

CONCLUSION

In this thesis the input and the radiation characteristics of an undulated line were studied. The model which is used throughout this thesis has a rectangular undulation form. The radiation patterns of this antenna, for different number of elements were calculated using an approximate expression for the array factor. The expression for this array factor was obtained using the concept of point source arrays. The validity of this approximate expression was tested by comparing its results with the numerical solution, using the NEC. This comparison showed that the simplified array factor can be used effectively to model the wire antenna, provided a proper attenuation constant is selected. It also indicated that the antenna elements generally resonate at a frequency which is higher than its physical resonance frequency, i.e., the frequency at which the undulation is one wavelength. Although the array factor approach is approximate, it helps in understanding the radiation mechanism of the antenna, which is generally unknown to date.

Since the radiation characteristics of this antenna depend on its geometrical dimensions, approximate design equations were obtained, based on the Taylor's line source distribution, to give the geometrical dimensions for a set of specified radiation char-

acteristics. The comparison of the near field pattern of the model obtained from these design equations with the theoretical Taylor distribution showed that the antenna elements toward the end radiate less enegry than the required Taylor distribution. The disagreement was thought to be due to phase error along the antenna, but when the phase error is corrected, then the near field distribution improves only slightly. The results obtained from this design which is based on these design equations is satisfactory, if one wants to obtain better improvement, an iteration method should be used.

Since this antenna is a travelling wave structure it should be matched to the load end to eliminate the reflection. Because of its three dimensional geometry, the determination of its characteristic impedance is difficult, which is further complicated by the presence of the dielectric substrate. To overcome this problem, the undulated line is normally connected to the load through a straight section of the line. The impedance matching at these terminals can therefore be achieved using the characteristic impedance of the straight portion of the line. This characteristic impedance was calculated numerically using the finite difference method. A computer program used to solve this method was prepared to calculate the line impedance for any trough and line shape, as well as to calculate the relative wave velocity of the strip. By controlling the thickness of the dielectric and the width of the strip, as well as the distance between the strip and the side walls, a wide range of characteristic impedance seems feasible.

In conclusion, it has been shown that the sandwich wire antenna can be designed approximately following the design procedure developed in this thesis. The results obtained demonstrate that satisfactory sidelobe levels can be obtained from this antenna.

APPENDIX

SPECIAL FINITE DIFFERENCE EQUATION

NO.	DESCRIPTION			FIGURE	CARTESIAN EQUATION
1	ORDINARY INTERIOR POINT			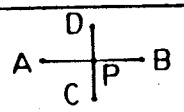	$\phi_A + \phi_B + \phi_C + \phi_D - 4\phi_P = 0$
2	ORDINARY POINT		BOTTOM EDGE	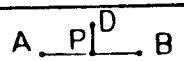	$\phi_A + \phi_B + 2\phi_D - 4\phi_P = 0$
3			TOP EDGE	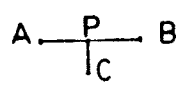	SIMPLE PERMUTATION OF (2)
4			LEFT HAND EDGE	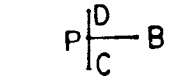	SIMPLE PERMUTATION OF (2)
5			RIGHT HAND EDGE	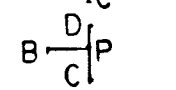	SIMPLE PERMUTATION OF (2)
6	CORNER POINT	BOTTOM	LEFT HAND SIDE	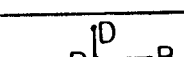	$\phi_B + \phi_D - 2\phi_P = 0$
7			RIGHT HAND SIDE	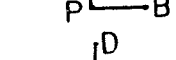	SIMPLE PERMUTATION OF (6)
8		TOP	LEFT HAND SIDE	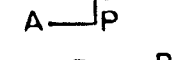	SIMPLE PERMUTATION OF (6)
9			RIGHT HAND SIDE	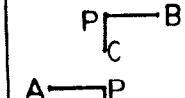	SIMPLE PERMUTATION OF (6)
10	DIELECTRIC INTERFACE	ROW INTERFACE	DIELECTRIC TO TOP	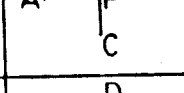	$(1+\epsilon_r)\phi_a + (1+\epsilon_r)\phi_B + 2\phi_C + 2\epsilon_r\phi_D - 4(1+\epsilon_r)\phi_P = 0$
11			DIELECTRIC TO BOTTOM	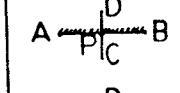	SIMPLE PERMUTATION OF (10)

APPENDIX

SPECIAL FINITE DIFFERENCE EQUATION

NO.	DESCRIPTION			FIGURE	CARTESIAN EQUATION
12		COLUMN INTERFACE	DIELECTRIC TO LEFT HAND SIDE	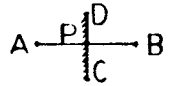	SIMPLE PERMUTATION OF (10)
13			DIELECTRIC TO RIGHT HAND SIDE	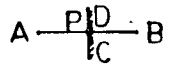	SIMPLE PERMUTATION OF (10)
14	ANGLE DIELECTRIC	ACUTE	FIRST QUADRANT	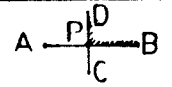	$2\phi_A + (\epsilon_r+1)\,\phi_B + 2\phi_C + (\epsilon_r+1)\phi_D - 2\,(\epsilon_r+3)\phi_P = 0$
15			SECOND QUADRANT	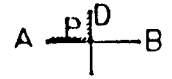	SIMPLE PERMUTATION OF (14)
16			THIRD QUADRANT	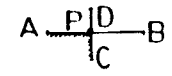	SIMPLE PERMUTATION OF (14)
17			FOURTH QUADRANT	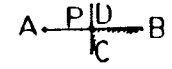	SIMPLE PERMUTATION OF (14)
18		OBTUSE	FIRST QUADRANT	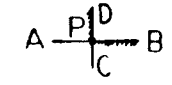	$2\epsilon_r\,\phi_A + (\epsilon_r+1)\phi_B + 2\epsilon_r\,\phi_C + (\epsilon_r+1)\phi_D - 2\,(3\epsilon_r+1)\phi_P = 0$
19			SECOND QUADRANT	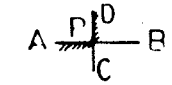	SIMPLE PERMUTATION OF (18)
20			THIRD QUADRANT	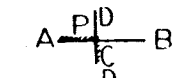	SIMPLE PERMUTATION OF (18)
21			FOURTH QUADRANT	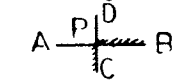	SIMPLE PERMUTATION OF (18)

APPENDIX

SPECIAL FINITE DIFFERENCE EQUATION

NO.	DESCRIPTION			FIGURE	CARTESIAN EQUATION
22	DIELECTRIC INTERFACE TO.	BOTTOM EDGE	DIELECTRIC TO LEFT HAND SIDE	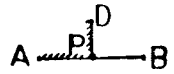	$\epsilon_r\phi_A + \phi_B + (\epsilon_r+1)\phi_D + 2(\epsilon_r+1)\phi_P = 0$
23			DIELECTRIC TO RIGHT HAND SIDE	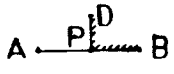	SIMPLE PERMUTATION OF (22)
24		TOP EDGE	DIELECTRIC TO LEFT HAND SIDE	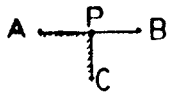	SIMPLE PERMUTATION OF (22)
25			DIELECTRIC TO RIGHT HAND SIDE	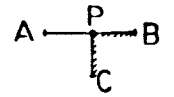	SIMPLE PERMUTATION OF (22)
26		LEFT HAND EDGE	DIELECTRIC TO TOP	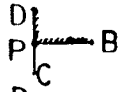	SIMPLE PERMUTATION OF (22)
27			DIELECTRIC TO BOTTOM	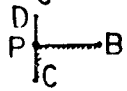	SIMPLE PERMUTATION OF (22)
28		RIGHT HAND EDGE	DIELECTRIC TO TOP	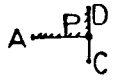	SIMPLE PERMUTATION OF (22)
29			DIELECTRIC TO BOTTOM	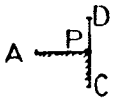	SIMPLE PERMUTATION OF (22)

REFERENCES

1. Rotman,W. and N. Karas. "The Sandwich Wire Antenna: new type of Microwave line source radiator," IRE Nat Conv Rec.,1, pt. 1,pp. 166-177, 1957.

2. ----------. " The sandwich wire antenna ," Microwave J., vol. 2, pp. 29-33, Aug. 1959.

3. Chen, k.M. "Sandwich Wire Antenna," IRE Trans. Antennas propag., vol. AP-10, pp. 159-164, March 1962.

4. Green, H.E. and Whittrow, J.L. " A New Analysis of the Sandwich Wire Antenna," IEEE Trans. Antennas Propag., vol. AP-19, No. 5, PP.600-605, Sept. 1971

5. Laverick, E. and Welsh, J. "Microwave Printed Circuit Aerial Research," Proc. Agard Conf., Nov. 1967, pp. 175-184.

6. Graham, R. and Dawson, C." A Sandwich wire Aerial," 1 st European Microwave Conf. London., Sept. 1969, pp. 528-531.

7. Hockham, G.A. and Wolfson, R.I., "Broadband Meander-Line Planar Array Antenna," IEE symp. Ant. & propag., 1979, pp. 645-647.

8. O. Aboul-Atta and L. Shafai "Hemispherically radiating Meander-Line planar array antenna," Third International Conference on Antennas and Propagation. ICAP 83, Norwich, England, Aprial 1983.

9. L .Shafai, "Sandwich Wire Antenna Design," DSS Contract No. 36001-2-0112, serial No. OST 82-00033.

10. Taylor, T.T., "Design of Line Source Antenna for Narrow Beamwidth and low sidelobe," IRE Trans. on Antennas & propag., vol. AP-3, pp. 16-28, Jan. 1955,

11. Graham, R. Doyle, M.F. Alexander, S.J. " Monopulse Aerials for Airbrone Radars," IEE Conference Publication. European Microwave Conference, London, pp. 362-366

12. James, Hall and Wood. " Microstrip antenna theory and design" Peter Peregrinus Ltd. (N.Y), 1981,

13. Grieg, D.D. and Engelmann, H.F. " Microstrip new Transmission Technique for the kilomegacycle Range," Proc. IRE, vol. 40, pp. 1644-1650 Dec. 1952,

14. Robert, M. Barrett " Microwave printed circuits- A historical survey IRE Trans. Microwave Theory and Techniques. MTT-No.2, pp. 1-9. March. 1955,

15. McDonough, J.A. Malech, R.G. and Kowabsky,"Recent Developments in the study of printed antennas," IRE National Convention Record, part 1, pp. 173-176, March. 1957,

16. Schneider, M.V. "Computation of impedance and attenuation of TEM-Lines by Finite Difference Methods," IEE Trans. on Microwave Theory and Techniques, vol. MTT-13, No. 6, pp. 793-800, Nov. 1965,

17. Green E. Harry. " The numerical solution of some important Transmission-Line problems," IEEE Trans. on Microwave Theory and Techniques. vol. MTT-13, No. 5, sept. 1965,

18. Korn, G.A. and Korn, T.M. "Mathematical Handbook for scientists and engineers," 1 st ed. (N.Y): McGraw-Hill, 1961

19. Southwell, R.V. "Relaxation Methods in theoretical physics," The Clarendon Press, Oxford, First Edition 1946

20. Martin, D.W. and Tee, G.J. " Iterative methods for linear equations With a symmetric positive definite matrix," The computer Journal. vol. 4, No. 3, pp. 242-254, Oct. 1961,

21. Franckel, S.P. " Convergence rates of iterative treatments of partial differential equations," M.T.A.C. vol. 4, pp.65-75

22. Carre, B.A. " The Determination of the optimum accelerating factor for successive over relaxation," The computer Journal, vol.4 No.1, pp. 73-78, 1961,

23. Reich, H.J. et al, "Microwave Theory and Techniques," 1st ed. (N.Y): Van Nostrand, sect. 1.3, ch.1, pp. 35, 1953,

24. Green, H.E. and J.R. Pyle, " The characteristic impedance and velocity ratio of dielectric-supported stripline," IEEE Trans. on Microwave Theory and Techniques (correspondence), vol. Mtt-13, pp. 135-137, Jan. 1965,

25. Green, H.E, "The characteristic impedance of square Coaxial line," IEEE Trans. on Microwave Theory amd Techniques (correspondence), vol. MTT-11, pp. 554-555, Nov. 1963,

26. Chon, S.B," Problem in strip transmission lines," IRE Trans. on Microwave Theory and Techniques, vol. MTT-3, pp. 119-126, March 1955,

27. Duncan, J.W. "A characteristic impedance of multiconductor strip transmission lines," IEEE Trans. on Microwave Theory and Techniques, vol. MTT-13, pp. 107-118, Jan. 1965,

28. Stibehelfer, H.E. " An accurate calculation of uniform microstrip transmission lines," IEEE Trans. Microwave Theory and Techniques, MTT-16, No. 7, pp. 439-443, july. 1968,

29. Warren, L. Stutzman and Gray, A. Thiele. " Antenna Theory and Design," John Wiely & Sons, Inc. 1981.

30. Ma, M.T. " Theory and application of antenna arrays," by John & Sons, Inc. 1974.

31. Numerical Electromagnetic Code (NEC) Part II: NEC Program Description- Code, Lawrence Livermore Laboratory, 1977.

32. Numerical Electromagnetic Code (NEC) Part III: NEC User's Guide Lawrence Livermore Laboratory, 1977,

33. Mittra, R., "Computer Technique For Electromagnetics," Pergamon Press, New York, 1973.